DEPARTMENT OF TRANSPORTATION

Use of J-Band to Improve the Performance of the HMA Longitudinal Joint

R. Christopher Williams, Principal Investigator
Asphalt Materials and Pavement Program
Institute for Transportation at Iowa State University

DECEMBER 2020

Research Project
Final Report 2020-33

To request this document in an alternative format, such as braille or large print, call 651-366-4718 or 1-800-657-3774 (Greater Minnesota) or email your request to ADArequest.dot@state.mn.us. Please request at least one week in advance.

Technical Report Documentation Page

1. Report No.	2.	3. Recipients Accession No.
MN 2020-33		

4. Title and Subtitle	5. Report Date
Use of J-Band to Improve the Performance of the HMA Longitudinal Joint	December 2020
	6.

7. Author(s)	8. Performing Organization Report No.
R. Christopher Williams, Joseph Podolsky and Joyce Kamau	

9. Performing Organization Name and Address	10. Project/Task/Work Unit No.
Asphalt Materials and Pavements Program Institute for Transportation Iowa State University 2711 South Loop Drive, Suite 4700 Ames, IA 50010-8664	11. Contract (C) or Grant (G) No. (c) 1003320 (wo) 6

12. Sponsoring Organization Name and Address	13. Type of Report and Period Covered
Minnesota Department of Transportation Office of Research & Innovation 395 John Ireland Boulevard, MS 330 St. Paul, Minnesota 55155-1899	Final Report 14. Sponsoring Agency Code

15. Supplementary Notes

http://mndot.gov/research/reports/2020/202033.pdf

16. Abstract (Limit: 250 words)

The density and air void content of asphalt mixtures affect the durability and performance of asphalt pavements. Pavement longitudinal joints typically have a lower density than the mat because they receive less compaction than the center section of the mat for various reasons. The higher air void percentages resulting from lower densities can lead to high permeability and allow water infiltration, which in turn can cause moisture-induced damage and decrease base and subbase support to the pavement, reducing pavement life. Void-reducing asphalt membrane (VRAM) has been used at the longitudinal joints of asphalt pavements to achieve higher densities and prevent moisture infiltration, thereby reducing deterioration at the longitudinal joints. VRAM is applied before the hot-mix asphalt (HMA) layer is placed and migrates into the HMA to fill 50% to 70% of the air voids.

This research evaluated the extent to which J-Band, a VRAM product, increases density and improves performance. Field cores were collected from two sections, one with and one without VRAM. Asphalt mixture performance tests, including disk compact tension and semi-circular bend tests, and push-pull tests were carried out in the laboratory on the field-collected specimens. Volumetric measurements were also taken, and ground penetrating radar was used in the field. It was determined that the pavement sections with VRAM had a lower permeability, higher bond energy, and higher fracture energy than the pavement sections without VRAM.

17. Document Analysis/Descriptors	18. Availability Statement
Air voids, Longitudinal joints, Fracture properties, Bonding and joining, Permeability, Asphalt pavements	No restrictions. Document available from: National Technical Information Services, Alexandria, Virginia 22312

19. Security Class (this report)	20. Security Class (this page)	21. No. of Pages	22. Price
Unclassified	Unclassified	61	

USE OF J-BAND TO IMPROVE THE PERFORMANCE OF THE HMA LONGITUDINAL JOINT

FINAL REPORT

Prepared by:

R. Christopher Williams
Joseph Podolsky
Joyce Kamau
Asphalt Materials and Pavements Program
Institute for Transportation at Iowa State University

December 2020

Published by:

Minnesota Department of Transportation
Office of Research & Innovation
395 John Ireland Boulevard, MS 330
St. Paul, Minnesota 55155-1899

ACKNOWLEDGMENTS

The authors would like to express their appreciation to the Minnesota Department of Transportation (MnDOT) for funding this project and specifically to the technical advisory panel and others: Eddie Johnson, Jerry Geib, Andrew Giesen, Josh Heck, Gregory Johnson, Charles Kremer, Clark Moe, Elliot Keyes, Kyle Hoegh, and Beth Klemann. Their input was invaluable to the researchers during the project and contributed to the quality of this report.

TABLE OF CONTENTS

LIST OF FIGURES

LIST OF TABLES

EXECUTIVE SUMMARY

Historically, hot-mix asphalt (HMA) pavements constructed in Minnesota typically have air void contents of about 7% to 8% in the mat and often approach or exceed air void contents of 10% at the longitudinal joints. Higher air void contents at the longitudinal joints can expose the pavement to premature deterioration and, as a result, compromise pavement integrity and performance. In Minnesota, the primary concern during asphalt pavement construction is the achievement of high density in the mixture, especially at the longitudinal joints. Valued at $29.5 billion, pavements have the largest replacement cost of all assets owned by the Minnesota Department of Transportation (MnDOT).

Void-reducing asphalt membrane (VRAM) has been used to achieve lower air void contents (higher densities) at the longitudinal joints of HMA pavements. VRAM, a highly polymer-modified asphalt membrane, is a composition comprised of an asphalt binder, an elastomeric polymer, and a wax modifier. The main component is the asphalt. The composition is applied at the longitudinal joints before the HMA layer is placed and migrates upward into the HMA layer to fill 50% to 70% of the air voids.

This research evaluated the use of J-Band, a commercially available VRAM product developed by the Heritage Research Group, to improve the performance of HMA longitudinal joints. Asphalt mixture performance tests were carried out in the laboratory on field-collected specimens, volumetric measurements were performed, and nondestructive field testing and field surveys were conducted. The properties of interest in the specimens were cracking resistance, migration and permeability, the bond to the existing surface, and the bond at the joint.

The laboratory specimens containing VRAM showed good performance in terms of having the highest joint bond energy, fracture energy, and work of fracture and good surface bond energy compared to the specimens without VRAM. The use of VRAM also reduces permeability and air void content, which reduces the intrusion of water into the pavement. The field surveys did not show any distress that is of concern. Based on the laboratory testing results, the use of VRAM improves the performance of the asphalt pavement mat at the longitudinal joints by protecting against deterioration caused by water and air infiltration.

CHAPTER 1: INTRODUCTION

Hot-mix asphalt (HMA) pavements historically constructed in Minnesota typically have air void contents of around 7% to 8% in the mat and often approach or exceed air void contents of 10% at the longitudinal joints. Mix density is very important in terms of its effects on the durability and performance of constructed pavements. Higher air void contents in the mat, especially at the longitudinal joints, lead to poor pavement durability. Poor durability is compounded because higher air void contents allow increased water infiltration, which leads to more required maintenance at longitudinal joint locations and can lead to the need for earlier reconstruction of the pavement. The infiltration of moisture into joints with higher air void contents also leads to reduced strength in the underlying pavement layers, which accelerates deterioration when the moisture in the pavement structure undergoes freeze-thaw cycling.

Previous research on longitudinal joints has shown that mixtures with lower air void contents (3% to 5%) are stronger and more durable than mixtures with air void contents of 7% to 10%. To achieve higher densities/lower air void contents in the mat at longitudinal joints, the Maryland joint construction method has been implemented in conjunction with an improved longitudinal joint density specification in Minnesota. However, density cores are not taken within 6 in. of the longitudinal joints in Minnesota, and that is where pavement deterioration often starts. Valued at $29.5 billion, pavements have the largest replacement value of all assets owned by the Minnesota Department of Transportation (MnDOT).

Void-reducing asphalt membrane (VRAM) is a hot-applied, highly polymer-modified asphalt membrane that extends the life of HMA longitudinal joints by migrating into 50% to 75% of the HMA void structure after rolling, thus reducing permeability at the joints and improving the mechanical performance of the mix at the joints through increased durability. The reduction in permeability minimizes water and air intrusion into the joints, resulting in reduced cracking and stripping and improved pavement performance. The improved mechanical performance is the result of increased amounts of polymer-modified asphalt within the mix at the longitudinal joints, which makes the mix more durable and less prone to cracking due to better recovery from loadings and increased bond strength. Extending the pavement life by one year saves MnDOT 5% per year in life-extension costs.

The research team used field-procured cores with and without J-Band, a commercially available VRAM product developed by the Heritage Research Group, to evaluate the extent to which VRAM improves the performance of the asphalt pavement mat at the longitudinal joints against deterioration due to water and air infiltration. The research included extensive laboratory testing of field cores as well as an evaluation of the improvements in durability and mechanical performance due to the increased bond strength resulting from the increased amounts of polymer-modified asphalt within the mix.

CHAPTER 2: LITERATURE

2.1 BACKGROUND

Research has been conducted to evaluate how construction practices impact the compaction of asphalt mixes in the field. This research has been geared towards enhancing compaction and thereby improving the durability of asphalt mixes and extending the service life of asphalt pavements (Blankenship 2015, Chang et al. 2014, Hekmatfar et al. 2015, Horan et al. 2012, Kassem et al. 2008, Masad et al. 2016, Masad et al. 2016, Sebaaly et al. 2008, Tran et al. 2016). However, the majority of this research was conducted with the goal of achieving higher densities after initial construction. None of the studies cited looked at the effects of the interaction between construction techniques and air void content on long-term pavement performance over a period of several years as indicated in field distress surveys. All of the studies focused on either short-term effects during or immediately after initial construction or life-cycle cost analysis (Blankenship 2015, Chang et al. 2014, Hekmatfar et al. 2015, Horan et al. 2012, Kassem et al. 2008, Masad et al. 2016, Masad et al. 2016, Sebaaly et al. 2008, Tran et al. 2016).

In Minnesota, the primary concern during asphalt pavement construction is the achievement of a sufficiently high density in the mat, especially at the longitudinal joints. A longitudinal joint is located at the interface between two parallel asphalt pavement mats. The choice of construction technique can affect the density immensely.

Previous research on longitudinal joints has shown that mixtures with lower air void contents (3% to 5%) are stronger and more durable than mixtures with air void contents of 7% to 10%. The infiltration of moisture into joints with higher air void contents also leads to reduced strength in the underlying pavement layers, thus accelerating deterioration when the moisture in the pavement structure undergoes freeze-thaw cycling.

It has also been shown from an N_{design} study conducted by Iowa State University for the Iowa Department of Transportation (DOT) that compacted mixtures with air void contents of 7% often do not achieve air void contents of 5% from traffic densification of the mix. N_{design} is the number of design gyrations for which an asphalt concrete specimen is compacted in the laboratory to achieve a certain air void content such that the mix design in the field will be able to achieve a lower air void content from initial compaction efforts during construction.

Historically, the main longitudinal joint construction techniques used in the United States include the use of echelon/tandem paving, various rolling patterns, various joint types (butt, tapered, and notched wedge), edge restraining or precompaction devices, infrared joint heaters, cutting wheels, joint adhesives, and joint sealers. Researchers at Purdue University indicated that in 2011 only 12 state DOTs (those not highlighted in orange in Figure 1, left) in the United States had specifications that included a longitudinal joint density requirement. This is shown in Figure 1 (left).

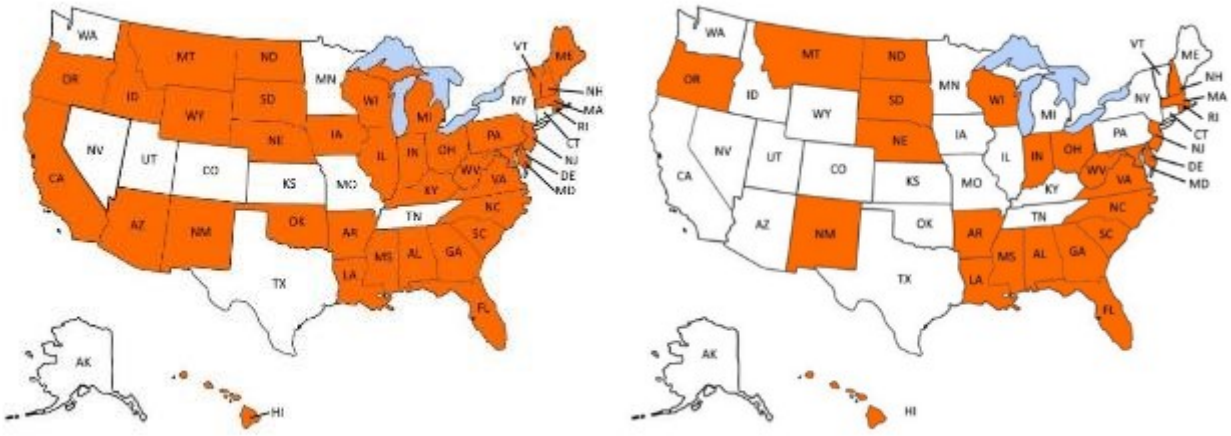

Sources: Kim 2017, McDaniel et al. 2012, Sebaaly and Barrantes 2004, Wang et al. 2016, Williams 2011, Zinke and Mahoney 2015

Figure 1. State DOTs without longitudinal joint density specifications (highlighted in orange) in 2011 (left) and 2018 (right)

By 2018, this number had increased to 24, as shown by the states not highlighted in orange in Figure 1 (right).

2.2 PRACTICES IN IOWA, WISCONSIN, AND MINNESOTA

In Iowa, several types of longitudinal joint construction techniques are used, such as the butt joint, notched wedge joint, modified butt joint with pinching, joint with heat treatment, and joint with edge restraint. Traditionally, contractors in Iowa have primarily used the butt joint, as shown in Figure 2.

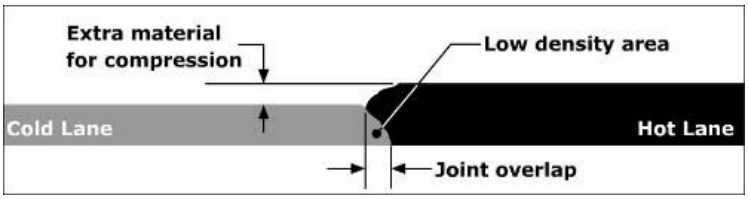

Pavement Interactive 2010 from WSDOT

Figure 2. Longitudinal butt joint

However, there is one issue with the butt joint, which is achieving an acceptable density for the unconfined edge of the cold lane. This occurs because there is no lateral confinement against the cold lane during compaction, and therefore the unconfined edge can move crosswise, making it difficult to achieve an acceptable density.

One way to correct for this issue is through pinching. In 2002, researchers from the National Center for Asphalt Technology (NCAT) in Auburn, Alabama, reported on how the modified butt joint with pinching increases the density at the longitudinal joint. Higher density was achieved by rolling from the hot lane (6 in.) away from the joint during the first pass so better confinement could be provided to the butt joint. Thus, material would be pushed between the roller and joint towards the joint during the initial

roller pass, causing pinching to occur and thereby producing a higher density at the butt joint area, as shown in Figure 3 (Kandhal et al. 2002).

Figure 3. Butt joint construction with hot pinch on US 61

Researchers in Canada found that tighter butt joints can be formed when using warm-mix asphalt (WMA) as opposed to HMA (Hughes et al. 2009).

Temperature plays an important role in longitudinal joint construction. Higher temperatures are believed to be better because compaction and bonding of the cold to hot mats can be improved at the joint. This is the basis of joint heat treatment, shown in Figure 4, in which the joint area is heated after placement of the cold lane or just prior to placement of the hot lane, which makes the asphalt binder in the cold lane more viscous and stickier.

Mark D. Blow 2017, Asphalt Institute

Figure 4. Infrared joint heaters

It has been reported that infrared heat can penetrate the existing pavement 25 to 50 mm into the joint and heat the asphalt mix to 60°C during the first pass of the roller. By the time of the last roller pass, the temperature will have decreased to 50°C (Daniel 2006). Results from field trials in Kentucky, Tennessee, and New Hampshire where joint heat treatment was used showed that permeability decreased, density increased, and indirect tensile (IDT) strength increased for all asphalt mixtures at the joints (Daniel 2006, Fleckenstein et al. 2002, Huang et al. 2010).

The notched wedge joint (shown in Figure 5) was originally developed by the Michigan Department of Transportation (MDOT) and has come to be recognized as a good method for longitudinal joint construction (Hasan et al. 2015).

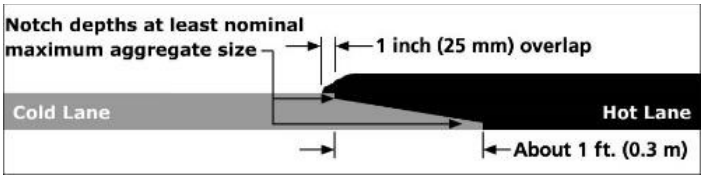

Pavement Interactive 2010 from WSDOT

Figure 5. Notched wedge joint

The notched wedge joint method is commonly used in Iowa and is the preferred method in Wisconsin when paving along unconfined edges during mainline paving. Otherwise, Wisconsin requires a full butt joint when paving adjacent to existing HMA pavement.

Buchanan (2000) compared the butt joint technique to the notched wedge joint technique on pavements in Colorado, Indiana, Alabama, Wisconsin, and Maryland. In-place densities were obtained from five pavement cores taken across the pavements' longitudinal joints: one at the centerline, two at 6 in. (150 mm) on either side of the centerline, and two at 18 in. (450 mm) on either side of the centerline. The results of this study indicated that the notched wedge joint can increase the in-place density of the asphalt mix at the longitudinal joint. However, in some cases it was observed that a decrease in in-place density did occur in the hot lane 6 in. (150 mm) from the joint when the notched wedge joint was used (Buchanan 2000). This could be due to construction-related problems because the same issue was later observed by other researchers in 2002 (Fleckenstein et al. 2002). The construction-related problems involved raveling on the lower portion of the wedge due to improper maintenance of the upper notch during compaction, which caused aggregate to be picked up by the small wedge roller. Additionally, notch bulging occurred in some cases.

In Iowa, longitudinal joints have also been constructed using milling operations to form edge restraints for both the cold and hot lanes. This is done by milling the cold lane to create a natural vertical edge face that acts as the edge restraint for the next new paving lane, as shown in Figure 6.

Brian Powell, NCAT

Figure 6. Milled lane on a pavement

After the new paving lane cools, the process is then repeated for the adjacent lane.

In 2014, MnDOT tasked asphalt contractors with improving density in the longitudinal joint. Their response was the Maryland joint method. In the Maryland joint method, the longitudinal joint is constructed such that there is a small overlap with the adjacent pavement lane. The overlap extends 1 in. to 1.5 in. onto the adjacent pavement lane and is about ¼ in. thick, as shown in Figure 7 (Minnesota Asphalt Pavement Association 2014).

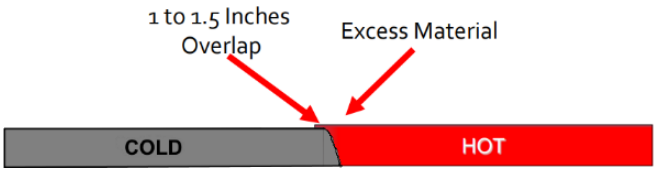

Adapted from Minnesota Asphalt Pavement Association 2014

Figure 7. Maryland joint method used in Minnesota

This is normally done with a butt joint, but some districts require a wedge joint. A joint heater has been used on a few projects.

2.3 LONGITUDINAL JOINT DENSITY SPECIFICATIONS IN IOWA AND MINNESOTA

2.3.1 Practice in Iowa

In Iowa, there are incentives for contractors to achieve a sufficient density at the longitudinal joint. Contractors must check the density of a pavement's longitudinal joint against developmental specification DS-15036. Random core locations are determined based on the number of daily field sub-lots within a mat. When there are three or more mat sub-lots, three locations are chosen at random for coring, while if there are fewer than three mat sub-lots, then only two locations are chosen for coring. If there are fewer than two mat sub-lots, then coring is waived. In addition, there are two different ways

of locating where cores are taken depending on whether the longitudinal joint is a butt joint or notched wedge joint. Coring diagrams for these two longitudinal joint types are shown in Figure 8.

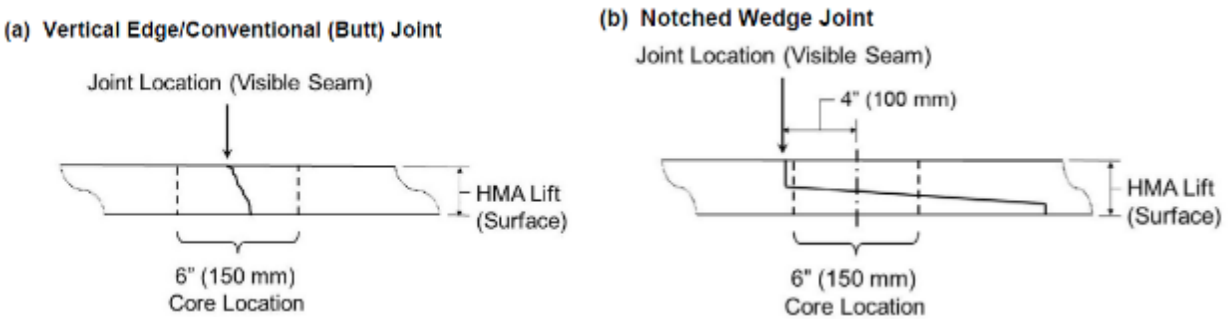

Iowa DOT 2015

Figure 8. Coring diagram for measuring longitudinal joint density for butt joints (left) and notched wedge joints (right)

In addition to the cores taken at the joint, cores need to be taken in the mat because in Iowa average joint density is determined as a percentage of average mat density, as shown in equation (1) (Iowa DOT 2015).

$$Avg\ Joint\ Density = 100 \times \frac{AvgJointG_{mb}}{AvgMatG_{mb}} \quad (1)$$

The rules that need to be followed for the coring process are that (1) mat cores and joint cores shall be collected on the same day of production for density determination and (2) mat cores identified as outliers for acceptable field air void contents will not be used to calculate average mat density. Based on the Avg Joint Density determined through equation (1), payment incentives and disincentives can be determined through Table 1.

Table 1. Payment for longitudinal joint density

Avg Joint Density (%)	Payment Adjustment ($/ft)
< 95.0[1]	0.16 × Avg Joint Density – 15.2
95.0 – 97.0	$0.00
> 97.0[2]	0.1333 × Avg Joint Density – 12.93

1. Disincentive is not to exceed $0.80/ft

2. Incentive is not to exceed $0.40/ft

Source: Iowa DOT 2015

2.3.2 Practice in Minnesota

In Minnesota, cores are taken from both sides of the mat such that the outer edge of the core is 6 in. from the longitudinal joint. Additionally, a companion core is taken 1 ft longitudinally from each of these cores, and two cores are taken to measure mat density at both 2 ft right and 2 ft left of the center of the mat. This is done once per 5,000 tons per day, with a minimum of one location per day. In Minnesota, the Total Pay Factor is determined by combining the effects of Pay Factors determined for mat density,

density in the longitudinal joint along the confined edge, and density in the longitudinal joint along the unsupported edge. Total Pay Factor can be determined in one of three ways (Minnesota Department of Transportaton 2016):

- Case 1: Total Pay Factor = (Pay Factor A) × (Pay Factor B) × (Pay Factor C)
- Case 2: Total Pay Factor = (Pay Factor A) × (Pay Factor B) × (Pay Factor B)
- Case 3: Total Pay Factor = (Pay Factor A) × (Pay Factor C) × (Pay Factor C)

Where Pay Factor A = Mat density, Pay Factor B = Confined edge density, and Pay Factor C = Unsupported edge density. A pay factor of 1.00 for Pay Factor B, Pay Factor C, or both is used in lots where no cores are taken at the longitudinal joint.

Tables 2 through 4 show all of the pay factors based on designed densities of 3% and 4% air voids for the mat, confined edge longitudinal joint, and unsupported edge longitudinal joint (MnDOT 2018).

Table 2. Payment schedule for maximum mat density

SP Wear and SP Shoulders (4% Void) Density, %*	SP Non-Wear and SP Shoulders (3% Void) Density, %*	Mat Density Pay Factor A	
		Traffic Level 2 & 3	Traffic Level 4 & 5
≥ 93.6	≥ 94.6	1.03**	1.05**
93.1 – 93.5	94.1 – 94.5	1.02**	1.04**
92.0 – 93.0	93.0 – 94.0	1.00	1.00
91.0 – 91.9	92.0 – 92.9	0.98	0.98
90.5 – 90.9	91.5 – 91.9	0.95	0.95
90.0 – 90.4	91.0 – 91.4	0.91	0.91
89.5 – 89.9	90.5 – 90.9	0.85	0.85
89.0 – 89.4	90.0 – 90.4	0.70	0.70
< 89.0	< 90.0	***	***

** Calculate the percent of maximum specific gravity to the nearest tenth.*

*** Payment will only apply if the weighted average air void content for the day's individual production falls within -½% of the target air void value. The weighted average air void content for each day is based on all of the mixture production tests conducted on that day in accordance with 2360.2.G.7, "Production Tests," with each test weighted by the tons of material that the test represents.*

**** MnDOT provides the following guidance: The Department will pay for the HMA material represented by the lot at 70% of the relevant contract unit price, unless a single core density is less than 87.0% of the maximum specific gravity (Gmm). If a single core density is less than 87.0% of Gmm, the Engineer will decide if the mixture is subject to removal and replacement or reduced payment at 50% of the relevant contract unit price. If the Engineer decides the material needs to be removed and replaced, the Contractor will remove and replace the material at no additional cost to the Department and will use other core samples to determine the limits of the removal and replacement area. Take additional core samples at the same offset from centerline as the original core. If the original low-density core was taken within 1½ ft (0.45 m) of an edge of the paver pass, take additional cores at 1½ ft (0.45 m) from the edge of the paver pass. Determine the densities at 50 ft (15 m) intervals both ahead and behind the point of unacceptable core density until finding a point of acceptable core density. If the incremental core density testing extends into a previously accepted lot, remove the unacceptable material. Do not use to the test results to recalculate the previously accepted lot density. Perform additional coring and testing for unacceptable core density at no additional cost to the Department. The Department will calculate the area of unacceptable pavement as the product of the longitudinal limits as determined by the 50 ft (15 m) cores and the full width of the paver pass, laying in the traffic lane or lanes. The Department will exempt shoulders from this calculation unless density failure occurred in the shoulder area. After removing and replacing the unacceptable material, determine the density of the replacement material by averaging the two cores. The Department will pay for the replacement material in accordance with Table 2360-22 or Table 2360-23. The Department will not pay for material removed. The Department will pay for the remainder of the original lot at 70% of the relevant contract unit price.*

Source: MnDOT 2018

Table 3. Payment schedule for longitudinal joint density (4% air voids)

Confined Edge Density (%) *	Pay Factor B (Longitudinal Confined Edge)		Unsupported Edge Density (%) *	Pay Factor C (Longitudinal Unsupported Edge)	
	Traffic Level 2 & 3	Traffic Level 4 & 5		Traffic Level 2 & 3	Traffic Level 4 & 5
≥ 92.1	1.02**	1.03**	≥ 91.0	1.02**	1.03**
91.6 – 92.0	1.01**	1.02**	90.1 – 90.9	1.01**	1.02**
89.5 – 91.5	1.00	1.00	88.1 – 90.0	1.00	1.00
88.5 – 89.4	0.98	0.98	87.0 – 88.0	0.98	0.98
87.7 – 88.4	0.95	0.95	86.0 – 86.9	0.95	0.95
87.0 – 87.6	0.91	0.91	85.0 – 85.9	0.91	0.91
< 87.0	0.85	0.85	< 85.0	0.85	0.85

** Calculate the percent of maximum specific gravity to the nearest tenth.*

*** Payment will only apply if the weighted average air void content for the day's individual production falls within -½% of the target air void value. The weighted average air void content for each day is based on all of the mixture production tests conducted on that day in accordance with 2360.2.G.7, "Production Tests," with each test weighted by the tons of material that the test represents.*

Source: MnDOT 2018

Table 4. Payment schedule for longitudinal joint density (3% air voids)

Confined Edge Density (%) *	Pay Factor B (Longitudinal Confined Edge)		Unsupported Edge Density (%) *	Pay Factor C (Longitudinal Unsupported Edge)	
	Traffic Level 2 & 3	Traffic Level 4 & 5		Traffic Level 2 & 3	Traffic Level 4 & 5
≥ 93.1	1.02**	1.03**	≥ 92.0	1.02**	1.03**
92.6 – 93.0	1.01**	1.02**	91.1 – 91.9	1.01**	1.02**
90.5 – 92.5	1.00	1.00	89.1 – 91.0	1.00	1.00
89.5 – 90.4	0.98	0.98	88.0 – 89.0	0.98	0.98
88.7 – 89.4	0.95	0.95	87.0 – 87.9	0.95	0.95
88.0 – 88.6	0.91	0.91	86.0 – 86.9	0.91	0.91
< 88.0	0.85	0.85	< 86.0	0.85	0.85

** Calculate the percent of maximum specific gravity to the nearest tenth.*

*** Payment will only apply if the weighted average air void content for the day's individual production falls within -½% of the target air void value. The weighted average air void content for each day is based on all of the mixture production tests conducted on that day in accordance with 2360.2.G.7, "Production Tests," with each test weighted by the tons of material that the test represents.*

Source: MnDOT 2018

VRAM has been used for the construction of HMA longitudinal joints in Illinois, Ohio, Iowa, Indiana, Michigan, and Missouri. VRAM is a composite material that consist of an asphalt binder, an elastomeric polymer, and a wax modifier. It can additionally include either a fumed silica or a fumed alumina or a saponified fatty acid and a resin acid gelling compound. The composition is modified to ensure that it does not flow before the placement of the HMA, and the wax modifier reduces the viscosity of the composition, allowing it to migrate. The composition loses its tackiness quickly on placement, allowing construction traffic to drive over the pavement within 15 to 30 minutes of placement.

VRAM migrates into the air voids in the asphalt pavement, filling up to 50% to 70% of them. The migration is due to heat of the mix and the compaction processes and is intended to reduce the number of interconnected air voids, decreasing the permeability and increasing the density of the pavement. VRAM can be used to resolve the problems associated with the high air void content of the asphalt mixture usually located within 9 in. of the longitudinal joint, making the pavement more structurally sound. VRAM can be applied underneath the HMA or at the vertical face of a constructed asphalt pavement mat (Kriech et al. 2016). Recommended application rates of VRAM according to a company that produces J-Band, a VRAM product, are shown in Table 5.

Table 5. VRAM application table for HMA mixes from a company that produces J-Band

Overlay Thickness (in.)	VRAM Width (in.)	Application Rate (lb/ft)
1	18	1.15
1¼	18	1.31
1½	18	1.47
1¾	18	1.63
2	18	1.80

2.4 EXPERIMENTAL METHODS FOR EVALUATING VRAM

2.4.1 Use of Ground Penetrating Radar in Determining Density in HMA

Ground penetrating radar (GPR) is a nondestructive, continuous, high-speed tool that has been historically used for mapping subsurface conditions for many applications, including highway systems, as shown in Figure 9 (Alongi et al. 1982, Morey 1998).

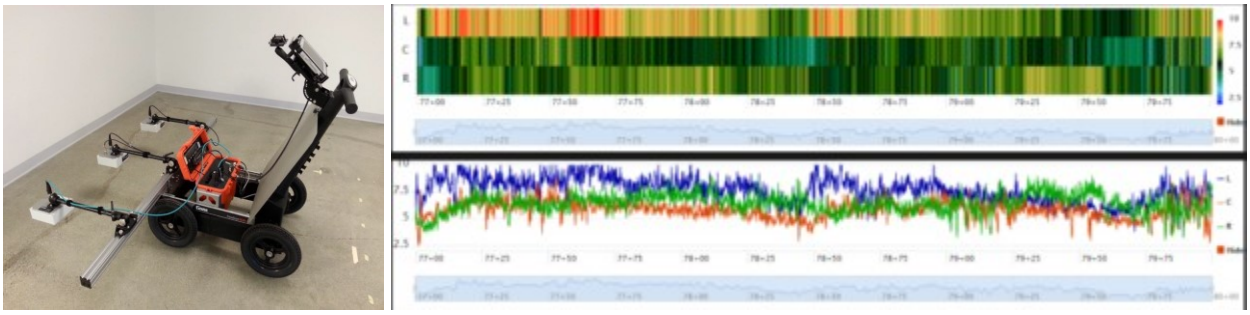

Khazanovich et al. 2017

Figure 9. Rolling density meter (a type of GPR) (left) and its resulting output (right)

GPR detects subsurface anomalies by mapping the changes in electromagnetic conductivity across material interfaces, making it a viable tool for detecting changes in pavement thickness, density, and, potentially, high-moisture areas. The use of GPR for highway systems gained increasing acceptance in the early 1990s (Attoh-Okine 1994, Buyukozturk and Rhim 1995, Fernando and Chua 1994, Les Davis et al. 1994, Scullion et al. 1992). GPR has continued to gain momentum as a tool for estimating density through nondestructive means in both the United States as well as other countries such as China,

Canada, Greece, and Portugal (Al-Qadiet al. 2010, Chen et al. 2014, Fernandes et al. 2017, Plati and Loizos 2013, Popik et al. 2010, Dai and Yan 2014).

In recent years, researchers from the University of Minnesota–Twin Cities, MnDOT, and the Federal Highway Administration (FHWA) conducted a study evaluating the use of GPR antenna array data to examine air void variations across an HMA mat. Through this research, it was shown that, instead of coring across the pavement at random locations, specific deficiencies could be found at particular locations and cores could be taken to further examine density at those locations. This work also provided a means of using GPR in one pass across a pavement without the need for core calibration (Hoegh et al. 2015). Research at the University of Illinois–Urbana-Champaign indicated that it is possible to use GPR on pavement with moisture on the surface. Through a correction algorithm, the researchers were able to minimize error significantly and still achieve density measurements with high accuracy (Shangguan et al. 2016).

However, identification of areas in the pavement with high volumes of water is another issue entirely. Researchers from Portugal recently showed that high-accuracy density measurements can be achieved in pavements that have up to 40% of their air void volumes filled with water, but identification of these areas and their locations in the pavement is still difficult due to the interconnectivity of air void systems inside asphalt mixes (Fernandes et al. 2017). Other works have looked at how moisture on the surface of a pavement would affect GPR after the pavement has been compacted in the field. Researchers from the Texas Transportation Institute and Texas A&M University–College Station were able to correlate high-density measurements from GPR with improved HMA performance in the laboratory using such tests as the Hamburg wheel tracking test, the indirect tensile strength test, and the Texas overlay test (Kassem et al. 2016).

The main interest in the present study was to determine whether VRAM, specifically a product called J-Band, enters as many voids as possible in the asphalt mat near the longitudinal joint. VRAM is a highly polymer-modified bituminous liquid-solid. Because GPR detects differences in density by measuring contrasts in electromagnetic conductivity across a material interface, it was felt that GPR would show how VRAM affects the density/air void content in an asphalt pavement at different pavement depths . It was also felt that GPR would show how far VRAM propagates upwards and downwards and whether the change is consistent across the region where the VRAM was laid (i.e., 9 in. to the right of the longitudinal joint).

2.4.2 Fluorescence Microscopy for use in Detecting Polymer Modification

An optical method used historically for observing how a polymer's structural network looks in polymer-modified asphalt is fluorescence microscopy (Handle et al. 2016, Kou et al. 2017, Lu et al. 1999, Lu et al. 2013, Mouillet et al. 2008, Polacco et al. 2015, Soenen et al. 2008, Zhu et al. 2017, Zhu et al. 2016). Even though the majority of studies using fluorescent microscopy have done so only for asphalt binder, three studies have looked at the effect of mixing and compaction on the morphology of the polymer-modified asphalt structure in asphalt mixes (Lu et al. 2010, Soenen et al. 2009, Wegan and Brule 1999). A study by Wegan and Brule (1999) found that the structure of pure polymer in the asphalt-aggregate matrix of a

polymer-modified asphalt mix was different than the structure of pure polymer in polymer-modified asphalt binder, as shown in Figure 10 (work done by the researchers at Iowa State University).

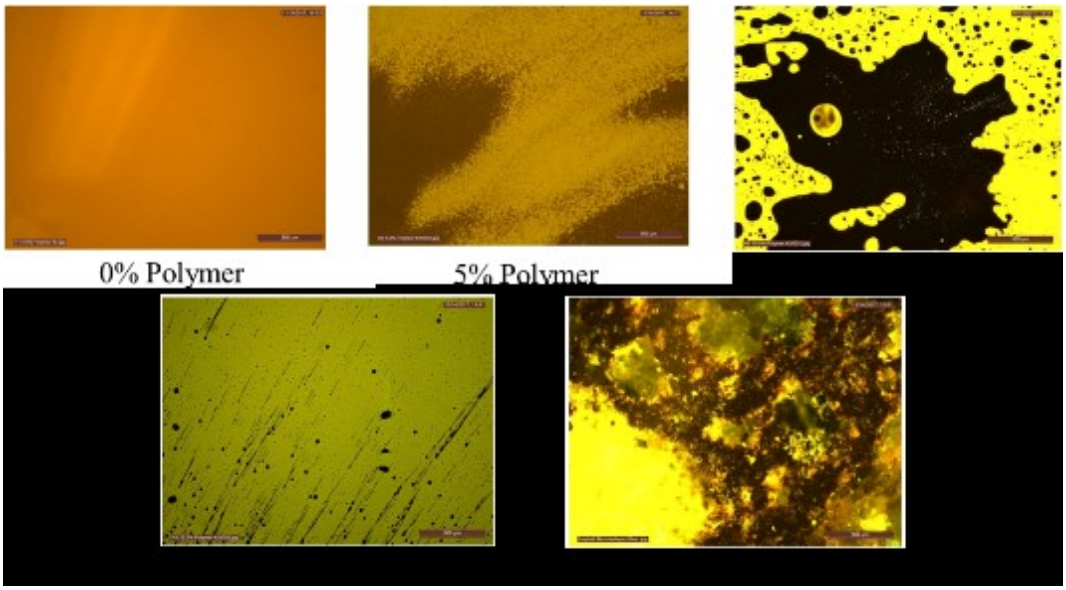

Figure 10. Fluorescence microscopy images showing changes in the polymer structural network of an asphalt binder as the percentage of polymer increases in a highly polymer-modified asphalt mix

It was also found that the affinity of a polymer to the mineral aggregates used in a mix is dependent on the aggregate types present, the polymer used, and the gradation of the aggregates.

The main interest in the present study was to determine whether VRAM, specifically a product called J-Band, enters as many voids as possible in the asphalt mat near the longitudinal joint. VRAM is a highly polymer-modified bituminous liquid-solid. In fluorescent microscopy, the asphalt binder, polymer, and aggregates in a mix will appear in different colors due to their fluorescence. Using fluorescent microscopy, it was felt that the effective penetration of polymer-modified VRAM towards the pavement surface could be identified at the point of application. It was also felt that fluorescent microscopy could be used to verify how far into the longitudinal joint VRAM penetrates under different paving conditions. Therefore, a procedure for preparing specimens similar to that used by Wegan and Brule (1999) was used to test and evaluate the polymer-rich asphalt-aggregate matrices created through the introduction of VRAM at longitudinal joints.

CHAPTER 3: MATERIALS AND METHODS

3.1 MATERIALS

3.1.1 Location of Field Site for Coring

The technical advisory panel (TAP) for this project worked with other MnDOT personnel and the paving industry to identify pavement locations meeting the traffic volume and length requirements for this research study. The study initially required asphalt pavement sections representing roads with low, medium, and high traffic volumes, with 1 mile of each section left untreated and 1 mile treated with J-Band. Due to the costs of VRAM, however, there was not enough material to pave 1-mile sections on roads with low and medium traffic volumes. Therefore, a 1-mile section treated with J-Band was paved on only one high-volume roadway, TH 22, and shorter treated sections were paved on the other roadway used for this study, US 169. Nevertheless, the project's objectives were achieved for TH 22 through the following:

- Paving a 1½ to 2 in. HMA overlay over an existing asphalt surface
- Prior to paving, applying an 18 in. width of VRAM at a rate according to the overlay thickness table recommendations in the area where the overlay centerline construction joint was placed
- Constructing a control section using the traditional joint construction method
- Sampling the HMA to determine binder and mix gradation

Control and J-Band sections, each 1 mile long, were paved in 2018 between CSAH 10 and CSAH 15 on TH 22 (SP 0704-100) north of Beauford. The J-Band section started at the driveway for Knewtson Soy Products LLP (latitude 44.0480, longitude -93.9577), shown in Figure 11, and ended just north of Decoria Cemetery (latitude 44.0614, longitude -93.9589) on the west side of TH 22.

Figure 11. Start of J-Band section at farm driveway

The control section started just north of Decoria Cemetery (latitude 44.0614, longitude -93.9589) and ended 1 mile farther north along TH 22 at latitude 44.0762, longitude -93.9559. The J-Band and Control sections are shown in Figure 12.

© Google Maps 2020

Figure 12. J-Band section (left) and control section (right)

Four sections were paved along US 169 in the following order: (1) 3,268 ft treated with VRAM, (2) 1,620 ft treated with VRAM and a preservation material produced by Crafco, (3) 1,346 ft of a control section, and (4) the remaining 7.9 miles (35,478 ft) of US 169 treated with a Crafco material. The first section started at latitude 43.679069, longitude -94.109093, and the last section ended at latitude 43.777166, longitude -94.165529 on US 169.

Coring was not done because the asphalt cores would have been less than 2 in. thick, making subsequent laboratory testing very difficult. Additionally, there was a rigid pavement underneath the new asphalt overlay that had been found to be experiencing alkali silica reactivity (ASR). ASR occurs when rigid pavement contains aggregates that are reactive with alkali, which causes cracking and deterioration to occur prematurely if water is present. Therefore, it was felt that taking up to 20 cores in each of the four sections on US 169 and refilling them with cold mix asphalt with high air voids would exacerbate the ASR issue and allow the deterioration in the base material for the asphalt overlay to propagate upwards.

3.2 METHODS

3.2.1 Laboratory Test Methods

Several methods have been used to measure and quantify the quality of longitudinal joint construction, including laboratory permeability tests, nuclear/non-nuclear density tests, core density tests, and ground penetrating radar (Chen et al. 2014). Previous studies in Arkansas, New England, and Tennessee have come to similar conclusions about the use of permeability tests to study longitudinal joints (Huang et al. 2010, Mallick and Daniel 2006, Williams et al. 2009). These findings were also confirmed in a longitudinal joint study that was recently completed in Iowa that resulted in a longitudinal joint density specification. All of these studies found that joints have significantly higher permeability compared to adjacent mats and that with the use of an infrared joint heater, permeability can be greatly reduced at longitudinal joints. However, none of these past studies have proposed quality control criteria using permeameters for longitudinal joint construction. Increased permeability significantly increases the rate of mix deterioration due to the higher potential for moisture-induced stripping and freeze-thaw damage.

Due to the importance of measuring permeability, in the present study falling head permeability tests were conducted in the laboratory on cored field specimens to measure the permeability of asphalt mixtures. The test procedure to evaluate the effectiveness of J-Band in reducing the permeability of longitudinal joints is outlined below:

- Take a minimum of six 6 in. cores from the VRAM section and six 6 in. cores from the control section. Three cores should be taken at the longitudinal joint from the centerline of the lane and three cores should be taken from the mat for the VRAM sections. Additionally, three cores should be taken next to the longitudinal joint centerline and three cores should be taken from the mat for the control sections.
- Freeze the cores and scrape the smeared VRAM from the outside of the cores.
- Cut the cores just below the interface of the VRAM or tack and the existing surface.
- Perform tests for bulk specific gravity (Gmb) on all cores.
- Perform 6 in. falling head permeability tests on all cores.
- Saw-cut each core at the mid-height of the overlay. Run falling head permeability tests on the top half and bottom half of all cores, as shown in Figure 13. The specimens used for laboratory testing in the present study were smaller in height than the recommended height of 50 mm.
- Break up the specimens to determine the actual specific gravity (Gmm).
- Use the Gmm and Gmb to determine the density/air void content of the cores.
- Perform extraction for asphalt content comparison of the top and bottom portions of the cores.

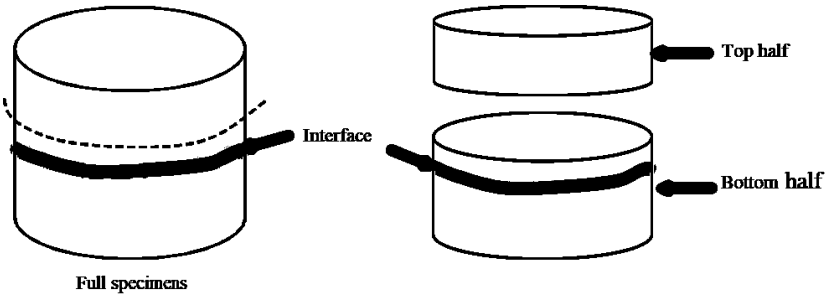

Figure 13. Falling head permeability samples

3.2.2 Low-Temperature Directional Bend Tests

Cracking resistance was measured through a low-temperature directional bend test similar to the single-edge notch test at low temperatures (Wagoner et al. 2005). The only difference was that for the evaluation of longitudinal joint construction with and without J-Band, the specimen size used was much smaller and closely aligns with the size of the specimens used in AASHTO TP 105-13 (AASHTO 2013, Exline et al. 2019). The test method is outlined below:

- Freeze the cores and scrape the smeared VRAM from the outside of the cores
- Cut the cores 1½ in. below the interface of the VRAM or tack and the existing surface, as shown in Figure 14
- Cut a notch below the VRAM within 5 mm of the interface
- Vary travel speed and temperature using Minnesota's current practice, as shown in Figure 15

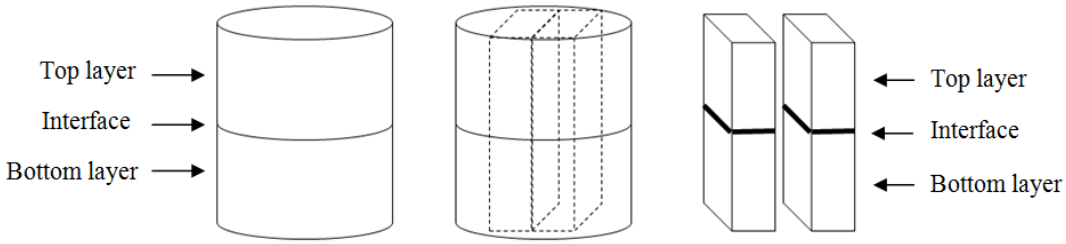

Marvin Exline, Heritage Research Group

Figure 14. Specimen preparation for low-temperature directional bend test

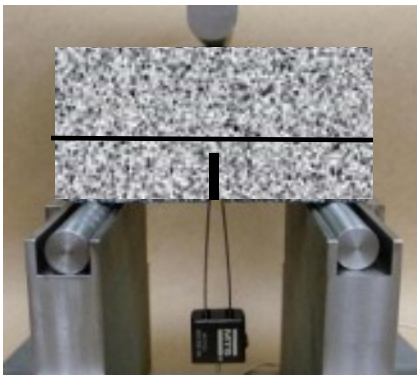

Marvin Exline, Heritage Research Group

Figure 15. Setup of low-temperature directional bend test with a specimen

In evaluating the low-temperature cracking resistance of the specimens, the disk-shaped compact tension (DCT) test was used with a travel speed 1.02 mm/min and the temperature set at the performance-grade (PG) low temperature + 10°C (ASTM 2013). However, the travel speed for the semi-circular bend (SCB) test described in AASHTO TP 105-13 is lower, at 0.3 mm/min, while the specimen size is almost the same and the direction of loading is the same as for the DCT test (AASHTO 2013, Wagoner et al. 2005). Therefore, the lower travel speed was used for this test.

3.2.3 Bond Energy Tests

Two test methods were used to measure bond energy, one for the surface and one for the joint. The method used for measuring bond energy at the surface is similar to the viscoelastic continuum damage (VECD) approach, except that instead of testing in push-pull mode with a uniaxial-sized (4 in. diameter by 6 in. height) specimen, the specimen was put through direct tension mode at a constant rate of 0.5 mm/min. The procedure for performing this test is outlined below:

- Take a minimum of six 4 in. cores from the VRAM section and six 4 in. cores from the control section at the longitudinal joint. The cores should be taken from the centerline of the lane for the VRAM sections and next to the longitudinal joint centerline for the control sections.
- Freeze the cores and scrape the smeared VRAM from the outside of the cores.
- Cut the cores ½ in. below the interface of the VRAM or tack and the existing surface.
- Run the universal testing machine (UTM) in direct tension mode at 4°C and a 0.5 mm/min loading rate, as shown in Figure 16.
- Calculate the bond energy at the surface.

Figure 16. Testing for bond surface energy in an asphalt mixture performance tester (AMPT): control sample with a normal bonding material (left) and sample containing VRAM layer (right)

The method used for measuring bond energy at the joint, the DCT test, is similar to the low-temperature cracking test. The procedure is outlined below, and a diagram of a test specimen is shown in Figure 17.

- Take a minimum of six 6 in. cores from the VRAM section and six 6 in. cores from the control section.
- Freeze the cores and scrape the smeared VRAM from the outside of the cores.
- Cut the cores approximately 5 mm below the interface of the VRAM or tack and the existing surface.
- Prepare the specimens in the configuration shown in Figure 17.
- Using the DCT test apparatus, test the specimens at -12°C and at a rate of 1 mm/min. For the present study, additional testing was also performed at a temperature of -24°C according to MnDOT's DCT procedure.
- Calculate the bond energy at the joint.

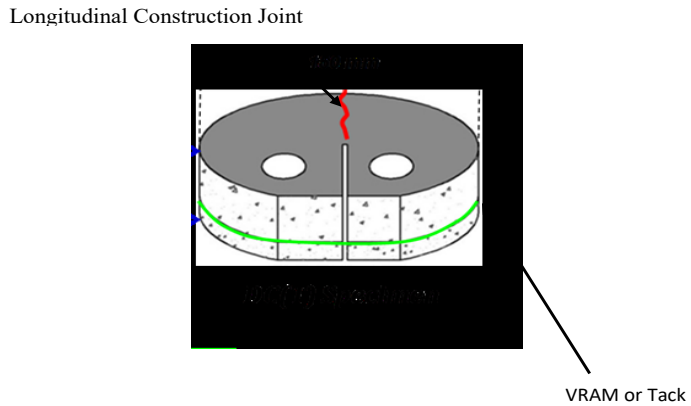

Marvin Exline, Heritage Research Group

Figure 17. Specimen for joint bond energy test

3.2.4 Fluorescence Microscopy for Use in Detecting VRAM Migration

Before the cores were scanned using a scanning electron microscope (SEM), an initial scan was carried out on binder samples to obtain the resolution and fluorescent colors to be expected. Overall, two stages of scanning were done for each sample:

1. Binder samples were scanned to characterize the binders. The binders used were the binder from the control sections; the binder from the VRAM sample, which was a mixture of the paving binder and the VRAM; and the VRAM binder obtained from the field cores. The samples were molded using a circular silicone mold used for viscosity rheometer sample preparation.
2. For each of the asphalt mixtures, two specimens with dimensions of 48 X 27 X 10 mm were scanned, one from the joint in the control section and the other from the joint in the VRAM-treated section. The specimens were cut from the top half of the samples used for permeability testing immediately above the transverse joint of the overlay.

3.2.5 Binder Performance Grade Determination

Binder was recovered from the field core samples using toluene, and distillation was done as per ASTM D7906. Dynamic shear rheometer testing was carried out as per AASHTO T 315-12 to obtain the PG high limit temperature of the binder. The samples were aged using a pressure aging vessel (PAV) according to ASTM D6521-08 and were then used for bending beam rheometer (BBR) testing in accordance with AASHTO T 313-12 to determine the value of the PG lower limit temperature.

3.2.6 Pavement Field Survey

During summer 2019, a field survey was conducted to evaluate the study sections' performance. The survey took place after the pavements had undergone one winter. During the survey, observations were documented and images were captured to support the observations.

CHAPTER 4: LABORATORY TEST RESULTS AND DISCUSSION

4.1 LABORATORY RESULTS

4.1.1 Mixture Performance

The VRAM samples had average joint bond energies of 902.5 J/m^2 and 1845.4 J/m^2 when tested at -24°C and -12°C, respectively, as shown in Figures 18 and 19.

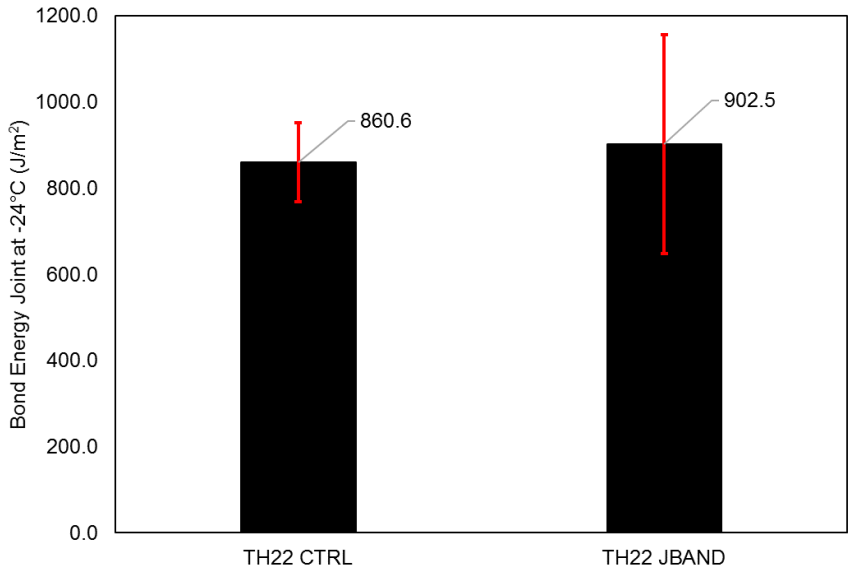

Figure 18. Joint bond energy results at -24°C

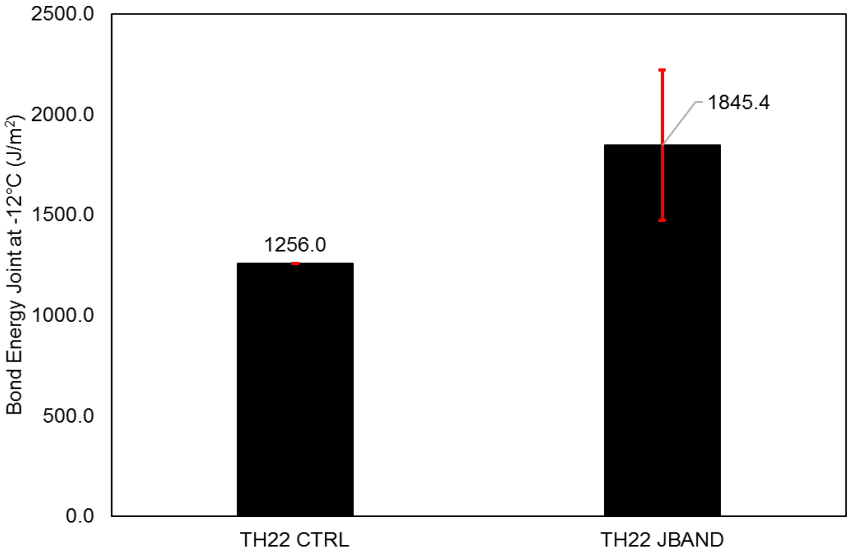

Figure 19. Joint bond energy results at -12°C

These average bond energies are higher than those of the control sections, with a greater difference observed between the samples from the control section and the VRAM-treated section at a test temperature of -12°C. The joint bond energies are higher at -12°C due to the binder becoming brittle at low temperatures and hence requiring less effort to cause cracking.

Similar to the results for the joint bond energy testing, the specimens from the VRAM-treated section have a higher surface bond energy compared to the specimens from the control section, as shown in Figure 20.

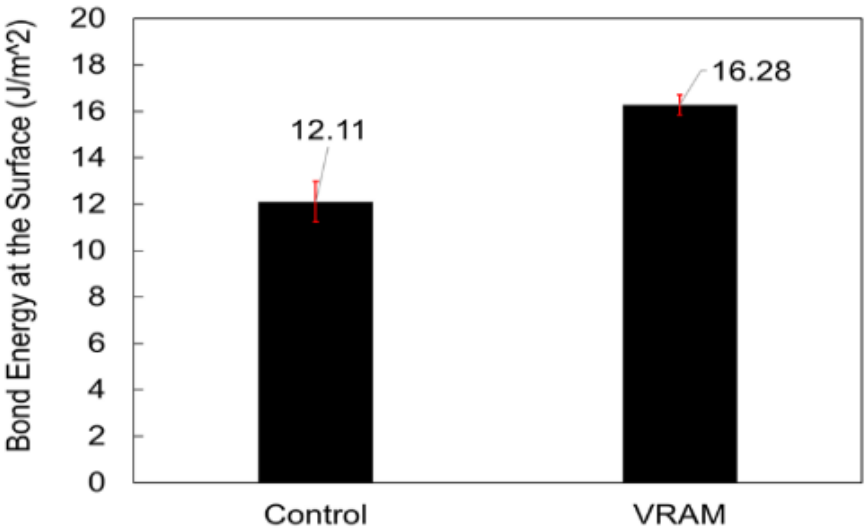

Figure 20. Surface bond energy result

The samples from the VRAM-treated section had an average surface bond energy of 16.28 J/m^2, while the samples from the control section had an average surface bond energy of 12.11 J/m^2. During the test, cracks formed above the surface of the bond for some of the samples containing VRAM. These results were obtained by a pull-apart test using a UTM in direct tension mode at 4°C and a 0.5 mm/min loading rate.

The cracking resistance measured for the VRAM-treated section was higher than the cracking resistance measured for the control section, as shown in Figure 21.

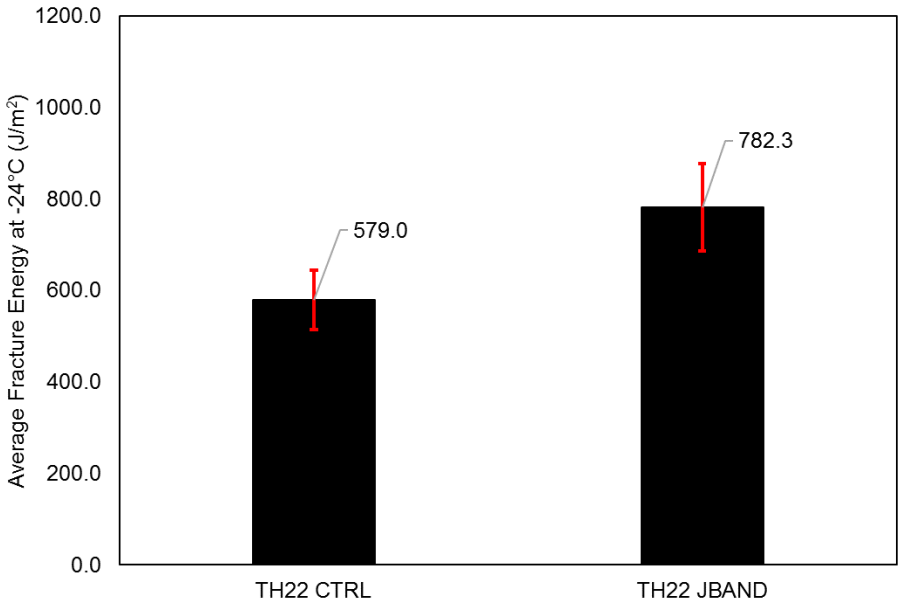

Figure 21. Cracking resistance results

The difference between the samples representing the two sections is 203.3 J/m^2, which shows a difference in the performance of the two sections.

Generally, the samples from the VRAM-treated section were observed to have higher joint bond energy, fracture energy, and surface bond energy than the samples from the control section, as shown in Figures 18 through 21. These three parameters indicate that fracture resistance may be improved through the use of VRAM in construction. The bond between the existing layer and the overlay could also be improved, as indicated by the surface bond energy results. Additionally, the joint bond between two adjacent lanes may be improved through the use of VRAM.

Table 6 shows the falling head permeability test results.

Table 6. Average permeability results for the full specimens and the top and bottom halves of the specimens

Specimen	Full	Top Half	Bottom Half
CTRL mat	5.9×10^{-5} cm/s	7.4×10^{-5} cm/s	5.3×10^{-5} cm/s
VRAM mat	6.8×10^{-5} cm/s	10.2×10^{-5} cm/s	11.9×10^{-5} cm/s
CTRL joint	10.6×10^{-5} cm/s	8.5×10^{-5} cm/s	5.9×10^{-5} cm/s
VRAM joint	0.0×10^{-5} cm/s	1.5×10^{-5} cm/s	0.0×10^{-5} cm/s

The permeability values obtained for the full specimens indicate that the specimen taken from the joint of the VRAM-treated section had zero permeability. However, it should be noted that there was a movement of water in the specimens to fill the few voids above the VRAM membrane. This was observed as a change in the water column height during the first 10 minutes of the test, followed by the value remaining constant for the final 20 minutes of test, with no water observed flowing out of the specimens. After cutting the specimens into two halves, the top half of the specimen taken from the joint of the VRAM-treated section had a permeability of 1.5×10^{-5} cm/s, which was much lower than that of the CTRL mat, VRAM mat, and CTRL joint for both the bottom and top halves. The bottom half of the

specimen taken from the joint of the VRAM-treated section had zero permeability because it still had the membrane layer.

The bottom half of the specimen taken from the joint of the VRAM-treated section had the lowest air void content and consequently zero permeability. The top half of this specimen had a permeability of 1.5×10^{-5} cm/s and an air void content of 6.4, which was the second lowest air void content. The specimens taken from the mat of the VRAM-treated section had the highest permeability values and lower air void contents than the bottom half of the specimen taken from the joint of the control section and top half of the specimen taken from the mat of the control section; this result is attributed to the how the air voids are distributed and connected in the different specimens.

The lower air void contents and zero permeability observed in the samples containing VRAM indicate that the use of VRAM reduces water intrusion and hence minimizes moisture-related deterioration, as shown in Tables 6 and 7.

Table 7. Average volumetric results for the full specimens and the top and bottom halves of the specimens

Specimen	Air voids (%)	Gmm	Gmb
Control joint bottom	7.1	2.434	2.260
Control mat top	6.6	2.435	2.273
VRAM mat top	6.6	2.424	2.264
Control mat bottom	8.6	2.453	2.241
VRAM joint top	6.4	2.400	2.247
Control joint top	6.9	2.446	2.277
VRAM mat bottom	7.0	2.437	2.267
VRAM joint bottom	5.7	2.315	2.184

Table 8 shows that the critical low temperatures for specimens ranged from -29.60°C to -27.59°C for a failure test temperature of -18°C and from -18.81°C to -29.31°C for a failure test temperature of -24°C.

Table 8. Binder performance grade and content results

Mixture name	Binder Content	Binder Grade	Critical Low Temp. (°C) Test Temp. -18°C	Critical Low Temp. (°C) Test Temp. -24°C	Critical High Temp. (°C)	MSCR Grade at 58°C
CTRL joint bottom	5.76	PG64-28	-27.59	-29.31	69.6	S
VRAM mat bottom	5.74	PG64-28	-27.59	-29.31	69.6	S
CTRL mat bottom	5.42	PG64-28	-27.59	-29.31	69.6	S
VRAM mat top	5.50	PG70-28	-28.21	-27.28	71.3	S
VRAM joint top	5.75	PG64-28	-29.60	-18.81	67.3	S
CTRL mat top	5.11	PG70-28	-28.21	-27.28	71.3	S
CTRL joint top	5.36	PG70-28	-28.21	-27.28	71.3	S
VRAM Joint bottom	9.56	PG70--28	-27.65	-28.94	72.4	V

The critical low temperature ranges were obtained by first aging and degassing the extracted and recovered binder of each group in a PAV and then conducting BBR tests at test temperatures of -12°C, -18°C, and -24°C. The bottom halves of the specimens had critical low temperatures ranging from -27.59°C to -29.31°C, while the top halves had critical low temperatures ranging from -18.81°C to -29.60°C. The top half of the specimen taken from the joint of the VRAM-treated section had an unusual critical low temperature based on a failure test temperature of -24°C, -18.81°C. This is most likely an outlier because the other samples' critical low temperatures ranged between -29.31°C and -27.28°C.

The virgin binder grade used during construction was PG58-34H for the overlay. However, after the binder was recovered for laboratory testing, the grading for the top halves of most of the specimens was PG70-28, while the specimen taken from the joint of the VRAM-treated section had a grade of PG 64-28. This difference may be an effect of the recycled asphalt pavement (RAP) used, and for the joint specimen the VRAM content may have changed the binder. For the bottom halves of most of the specimens, the binder grade was PG 64-28. The specimen taken from the joint of the VRAM-treated section had a grade of PG 70-28, which could also have been a result of the VRAM content.

4.1.2 Fluorescence Microscopy

The initial scan of the binders described in Section 3.2.4 was used to pre-identify the differences expected in the colors of the different samples. The VRAM binder sample contained traces of minerals associated with the mineral fillers in the asphalt mix, possibly because obtaining this binder involved scraping the sample from a cored field sample. No difference in the image colors between the VRAM and control samples was observed, as shown in Figures 22 and 23. This was linked to the possibility that all of the VRAM binder sample could have been modified.

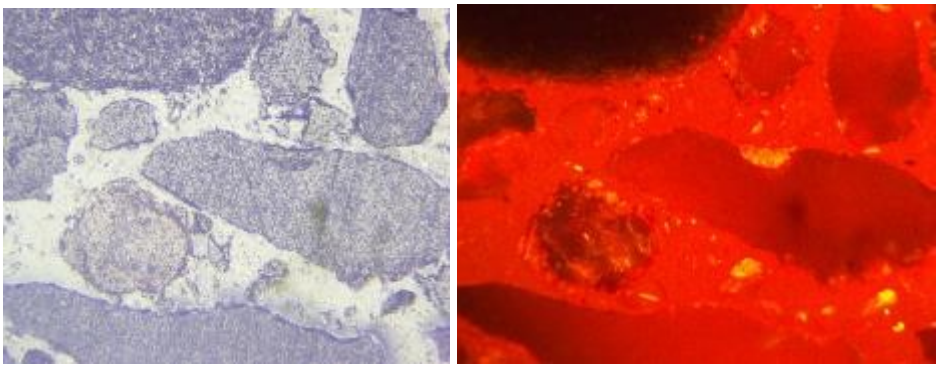

Figure 22. VRAM mixture: black and white (left) and UV (right)

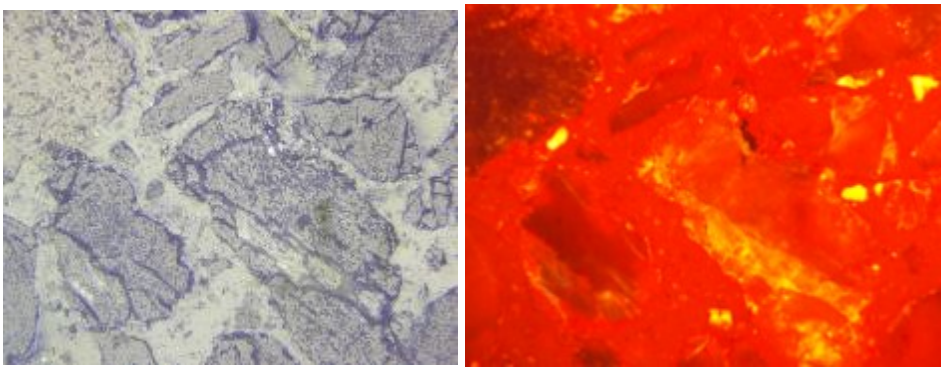

Figure 23. Control mixture: black and white (left) and UV (right)

There were differences in color at the edges of some of the aggregates. However, this may be because some of the aggregates fluoresce due to the different minerals they contain. There is a need for thinner sections to do fluorescent microscopy by transmittance instead of reflectance. However, obtaining thinner sections (25 to 30 µm) is very difficult because the binder smears over the aggregates due to the heat generated from the friction of the polishing equipment and because of aggregate cracking, rendering the sample glass-like.

4.2 FIELD SURVEY DATA ANALYSIS AND CORRELATION TO LABORATORY PERFORMANCE RESULTS

4.2.1 Field Survey

A field performance survey of TH 22 just north of Beauford, Minnesota, was carried out on October 25, 2019, one year after construction was finished. The pavement section made with J-Band did not show any noticeable distresses at the longitudinal joint, as shown in Figure 24.

Figure 24. VRAM section on TH 22 between the cemetery near 179th Street and 169th Street

The control section (without VRAM) on TH 22 also did not show any noticeable distresses at the longitudinal joint, as shown in Figure 25.

Figure 25. Control section on TH 22 north of the cemetery near 179th Street

In both the control and VRAM pavement sections, minor amounts of raveling were observed in the middle of the mat between the wheel paths. Because there were no noticeable distresses (primarily longitudinal joint cracking) within 9 in. of each side of the longitudinal joint, it was not possible to make correlations between field performance and laboratory performance after only one year. More time is needed to differentiate the J-Band sections from the control sections in terms of field performance.

4.2.2 Ground Penetrating Radar Results

GPR was used in the mat and joint areas of both the control and VRAM sections on TH 22 to obtain the density of the pavement by measuring the surface reflection amplitude to determine the approximate dielectric constant.

From observing the dielectric constant data shown in Figures 26, 27, and 28, it can be seen that the pavement mats have higher dielectric constant values than the joints.

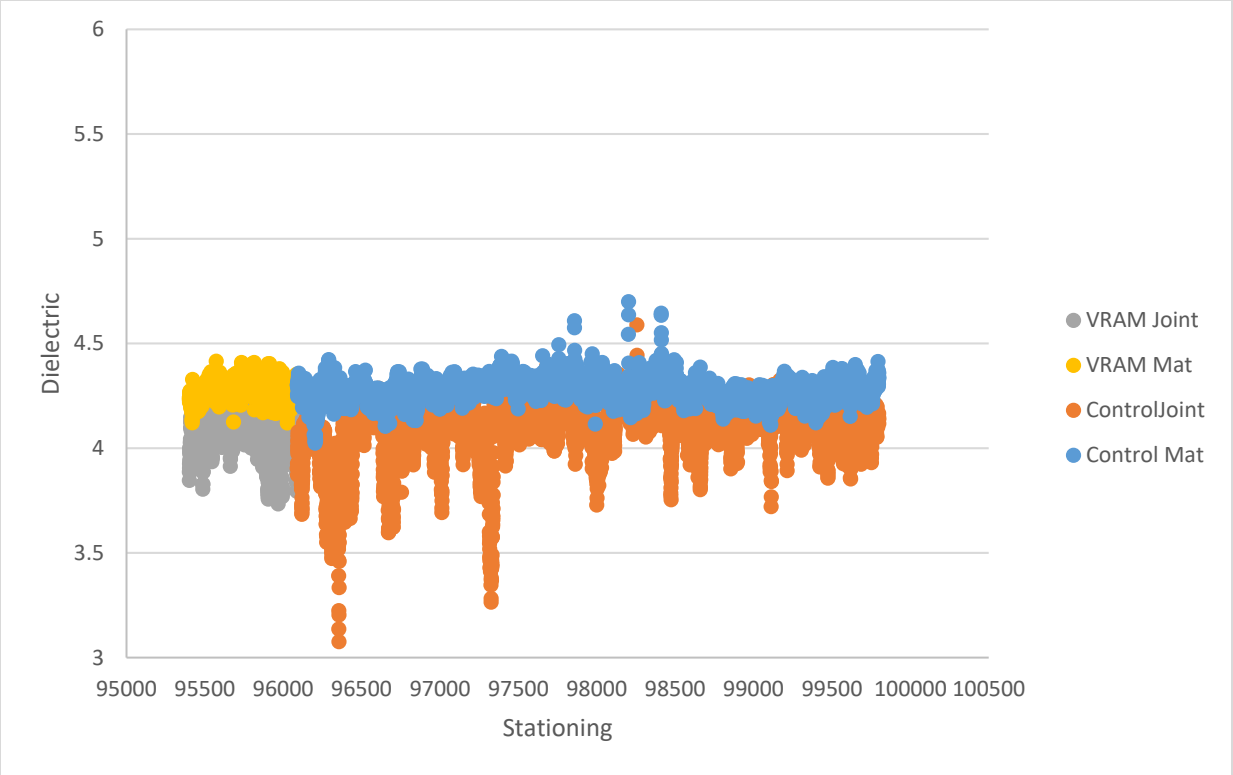

Figure 26. Dielectric constant data for TH 22

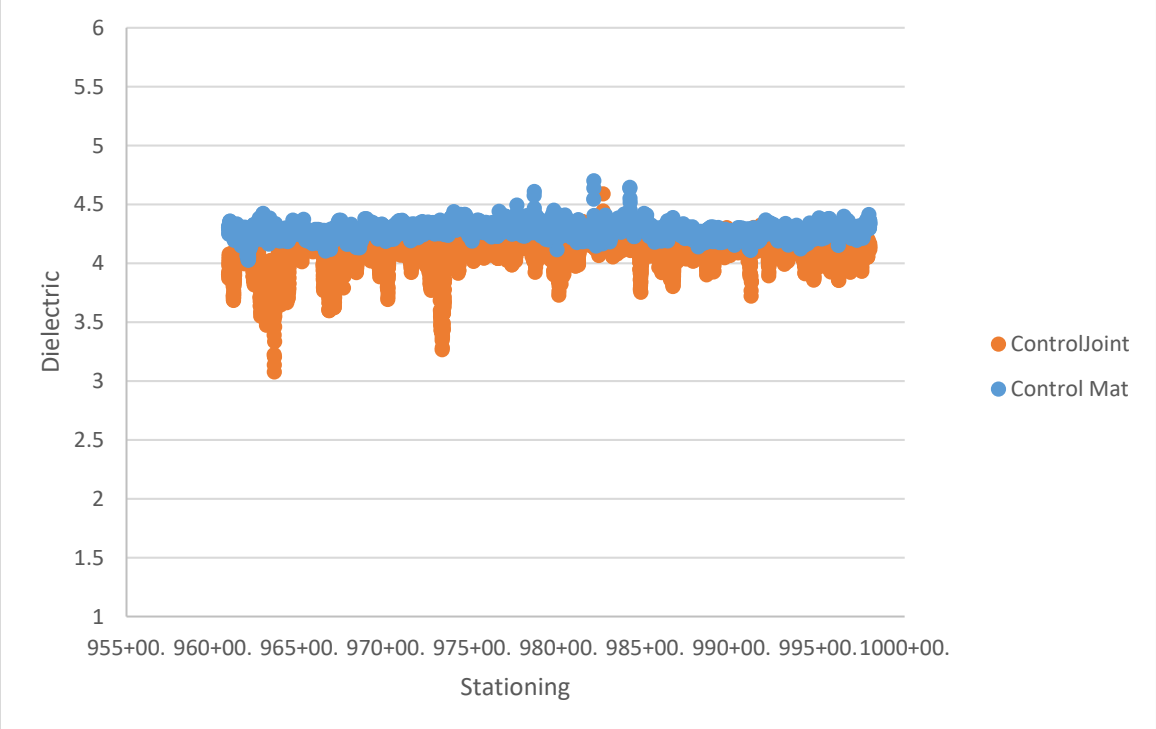

Figure 27. Dielectric constant data for the control pavement section

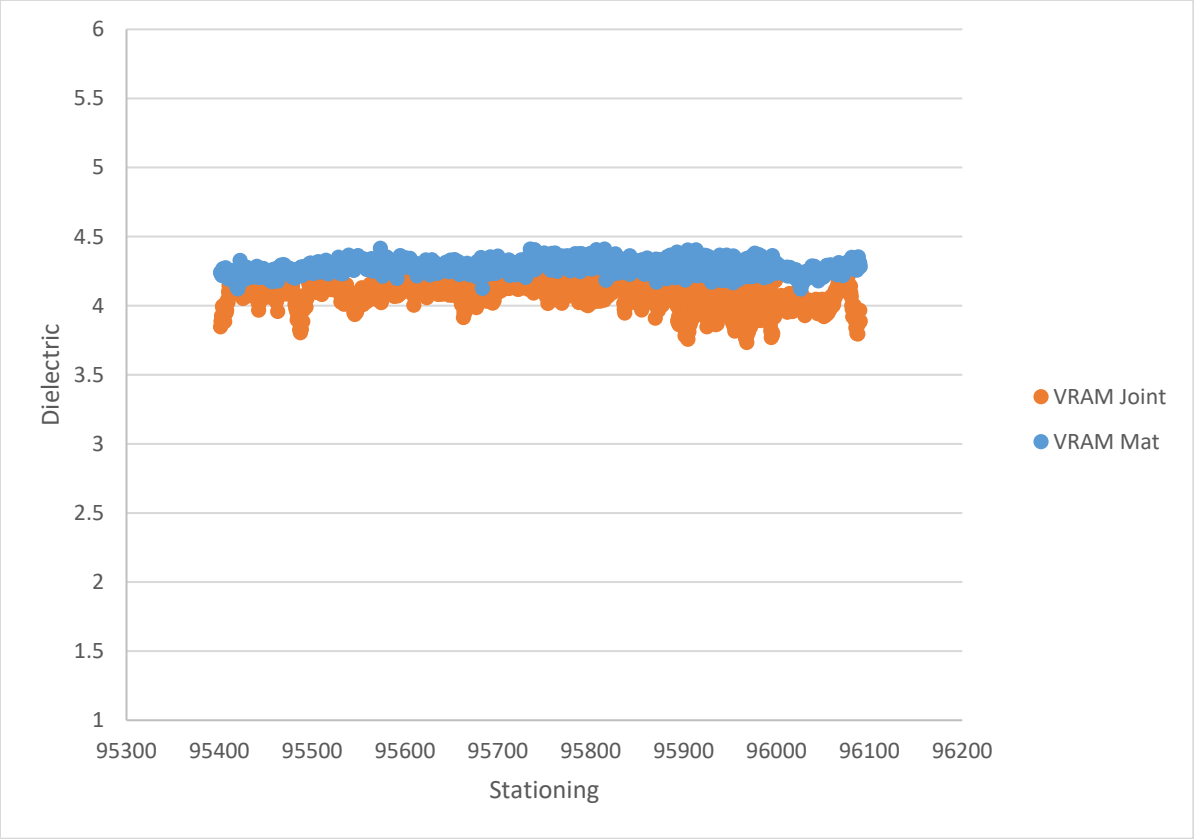

Figure 28. Dielectric constant data for the VRAM pavement section

Past literature shows that lower dielectric constant values indicate higher air void contents/lower densities in the pavement. Thus, the values collected through GPR correlate well to what has been shown in past literature (Hoegh and Dai 2017, Hoegh et al. 2018, Hoegh et al. 2015, Hoegh et al. 2019, Hoegh et al. 2020). However, it can be inferred based on the results that VRAM has a positive impact in terms of increasing the pavement density/lowering the percent air voids because the dielectric constant values obtained at the joint are much closer to the values obtained at the mat in the VRAM section than they are in the control section.

The GPR results were not calibrated to the mix because static measurements must be made at the exact locations where cores are taken or puck calibration based on dielectric constant measurement of the produced mix at various air void contents is required, while the field cores used to determine air void contents in the laboratory were taken at different locations than where GPR was used because coring was not done in conjunction with GPR. Even though the measurement lengths in the VRAM section were shorter than those in the control section, several lengths in the control section that are equal in proportion to the lengths in the VRAM section show much more variation.

While the GPR measurements obtained in this study correlate well with what the literature has indicated VRAM should do to the pavement, the volumetric data obtained in the laboratory for the field cores do not agree with literature. The air void percentages obtained for each section's cores do not correlate with the dielectric constant values as per the literature. The mat sections were found to have

higher average air void percentages than the joint sections, which should indicate lower dielectric constant values for the mats than the joints, which is not the case. The VRAM joint was found to have an air void content of 6.1% while the corresponding mat was found to have an air void content of 6.7%, which is higher than that of the joint. Using the dielectric constant, we would expect the air void content to be higher in the joint than in the mat, but this is not the case.

CHAPTER 5: CONCLUSIONS AND RECOMMENDATION

5.1 CONCLUSIONS

From this study, the following can be concluded:

1. The field cores containing VRAM showed better results in the laboratory than the cores taken from the control section in that they have the highest joint bond energy, fracture energy, and work of fracture and good surface energy. The high surface and joint bond energies indicate that longitudinal cracking at the joints will be delayed relative to the control sections because more energy will be needed for cracking to occur. Cracking resistance at the joint may also have been improved, as shown by the high fracture resistance value.
2. The use of VRAM also reduces permeability and air void content, which reduces the intrusion of water into the pavement, indicating that good long-term pavement performance will be achieved. The permeability of an asphalt mixture always depends on its macrostructure. When VRAM migrates into the hot overlay, it fills the air voids, altering the macrostructure of the HMA overlay.
3. The one-year field survey did not show any distress that was of concern; however, more time will be needed to see if J-Band offers any performance benefits based on field performance.

Generally, it can be concluded that the use of VRAM improves the performance of the asphalt pavement mat at the longitudinal joints because it reduces permeability and lowers air void content, thereby protecting against deterioration (i.e., cracking and stripping) caused by water and air infiltration. Improved performance in terms of cracking resistance was also evident because the VRAM section was found to have higher fracture resistance and higher surface and joint bond energies than the control section.

The fluorescence microscopy test results are inconclusive because some of the aggregates fluoresce due to the different minerals they contain, making analysis difficult. There is a need for thinner sections to perform fluorescent microscopy by transmittance instead of reflectance.

5.2 RECOMMENDATIONS

1. There is need for a future study that includes more sections to offset the variabilities caused by different construction methods, different PG binders used for different sections, different overlay thicknesses, and variations in other materials used.
2. A study on bond energy could be done comparing cores that contain VRAM to cores that contain other types of materials to further evaluate the improvement in bond energy through VRAM.
3. To better measure field performance, field distress surveys should be conducted annually for approximately five years after construction to obtain an accurate analysis and correlations with the performance of the study sections used in this research.

5.3 POTENTIAL BENEFITS

The benefits from this project can be realized through the implementation of VRAM. The increased initial material cost for asphalt paving due to the use of VRAM is anticipated to be substantially offset by the material savings that would result from extended pavement life and reduced costs for routine maintenance. In addition, if VRAM is used in bulk, the cost is reduced to $12,500 per mile from $15,000 per mile, which was the initial cost of the VRAM used in this project. A producer of VRAM has confirmed this price break, and the cost of VRAM in Illinois has been approximately $12,250 per mile.

If the resistance to cracking observed in the laboratory portion of this research is translated into the pavement sections in the field, then cracks are anticipated to appear earlier in the control sections than in the VRAM-treated sections. This means that maintenance activities would be needed more often in the control sections than the VRAM-treated sections and therefore that the VRAM-treated sections will last longer and require much fewer maintenance activities over the course of their lives. With more years of service, the VRAM-treated sections will accrue more cost savings than the control sections. Thus, the use of VRAM can be considered as preventive maintenance that occurs during initial construction, in that it reduces the need for routine maintenance.

VRAM could be used where impermeable barrier materials are required. For example, coring was ruled out in one of the field sections due to the risk of alkali-silica reactivity in the presence of water, indicating that this section requires waterproofing. However, a study should first be done on the use of VRAM as an impermeable barrier material. Promising signs of this potential use were observed during the falling head permeability tests for the samples that had a VRAM membrane, which were found to have zero permeability.

REFERENCES

AASHTO. 2012. *AASHTO T 313-12 Standard Method of Test for Determining the Flexural Creep Stiffness of Asphalt Binder Using the Bending Beam Rheometer (BBR*). American Association of State Highway and Transportation Officials, Washington, DC.

AASHTO. 2012. *AASHTO T 315-12 Standard Method of Test for Determining the Rheological Properties of Asphalt Binder Using a Dynamic Shear Rheometer (DSR*). American Association of State Highway and Transportation Officials, Washington, DC.

AASHTO. 2013. *AASHTO TP 105-13 Standard Method of Test for Determining the Fracture Energy of Asphalt Mixtures using the Semicircular Bend Geometry (SCB*). American Association of State Highway and Transportation Officials, Washington, DC.

Al-Qadi, I. L., Leng, Z., Lahouar, S., and Baek, J. 2010. In-Place Hot-Mix Asphalt Density Estimation using Ground-Penetrating Radar. *Transportation Research Record: Journal of the Transportation Research Board,* No. 2152, pp. 19–27.

Alongi, A., Cantor, T., Kneeter, C., and Alongi Jr, A. 1982. Concrete Evaluation by Radar Theoretical Analysis. *Transportation Research Record: Journal of the Transportation Research Board,* No. 853, pp. 31–37.

ASTM. 2008. *ASTM D6521 - 08 Standard Test Method for Determining Fracture Energy of Asphalt-Aggregate Mixtures Using the Disk-Shaped Compact Tension Geometry*. ASTM International, West Conshohocken, PA.

ASTM. 2013. *ASTM D7313 - 13 Standard Test Method for Determining Fracture Energy of Asphalt-Aggregate Mixtures Using the Disk-Shaped Compact Tension Geometry*. ASTM International, West Conshohocken, PA.

ASTM. 2014. *ASTM D7906 - 14 Standard Practice for Recovery of Asphalt from Solution Using Toluene and the Rotary Evaporator*. ASTM International, West Conshohocken, PA.

Blow, M. D. 2017. *Best Practices for Constructing and Specifying HMA Longitudinal Joints*. Longitudinal Joint Workshop Series. Asphalt Institute and FHWA.

Attoh-Okine, B. 1994. *Using Ground Penetrating Radar as an Integral Part of the Formulation of Maintenance Decisions concerning Flexible Pavements*. Paper presented at the Fifth International Conference on Ground Penetrating Radar, Kitchener, ON, Canada.

Blankenship, P. 2015. Improving Pavement Density. *Asphalt,* Vol. 30, No. 3, pp. 29–32.

Buchanan, M. 2000. Evaluation of Notched-Wedge Longitudinal Joint Construction. *Transportation Research Record: Journal of the Transportation Research Board,* No. 1712*,* pp. 50–57.

Buyukozturk, O., and Rhim, H. C. 1995. *Radar Imaging of Reinforced Concrete Specimens for Nondestructive Testing.* Paper presented at the Nondestructive Evaluation of Aging Bridges and Highways, Oakland, CA.

Chang, G., Xu, Q., Rutledge, J., and Garber, S. 2014. *A Study on Intelligent Compaction and In Place Asphalt Density*. FHWA-HIF-14-017. Federal Highway Administration, Office of Pavement Technology, Washington, DC. https://rosap.ntl.bts.gov/view/dot/38554.

Chen, D.-H., Hong, F., Zhou, W., and Ying, P. 2014. Estimating the Hotmix Asphalt Air Voids from Ground Penetrating Radar. *NDT and E International,* Vol. 68 (Supplement C), pp. 120–127.

Dai, S. and Yan, A. Q. 2014. *Pavement Evaluation Using Ground Penetrating Radar*. Paper presented at the Geo-Shanghai 2014: Pavement Materials, Structures, and Performance, Shanghai, China.

Daniel, J. S. 2006. Use of an Infrared Joint Heater to Improve Longitudinal Joint Performance in Hot-Mix Asphalt Pavements. *Journal of Performance of Constructed Facilities,* Vol. 20, No. 2, pp. 167–175.

Exline, M. K., Cunningham, J. J., and Kriech, A. J. 2019. *Apparatus and Method for Applying Asphalt Binder Compositions including Void Reducing Asphalt Membrane Compositions for Paving Applications*. U.S. Patent No. 10,465,345. United States Patent and Trademark Office, Washington, DC.

Fernandes, F. M., Fernandes, A., and Pais, J. 2017. Assessment of the Density and Moisture Content of Asphalt Mixtures of Road Pavements. *Construction and Building Materials,* Vol. 154, pp. 1216–1225.

Fernando, E. G., and Chua, T.-S. 1994. *Development of a Route Segementation Procedure Using Predicted Layer Thicknesses from Radar Measurements.* Paper presented at the Fifth International Conferention on Ground Penetrating Radar, Kitchener, ON, Canada.

Fleckenstein, L. J., Allen, D. L., and Schultz, Jr., D. B. 2002. *Compaction at the Longitudinal Construction Joint in Asphalt Pavements*. Kentucky Transportation Center, Lexington, KY.

Handle, F., Füssl, J., Neudl, S., Grossegger, D., Eberhardsteiner, L., Hofko, B., Hospodka, M., Blurb, R., and Grothe, H. 2016. The Bitumen Microstructure: A Fluorescent Approach. *Materials and Structures,* Vol. 49, pp. 167–180.

Hasan, M. R. M., Porter, D., and You, Z. 2015. Synthesis of Longitudinal Joint of Flexible Pavement. *Jurnal Teknologi,* Vol. 73, No. 4, pp. 7–14.

Hekmatfar, A., McDaniel, R. S., Shah, A., and Haddock, J. E. 2015. *Optimizing Laboratory Mixture Design as it Relates to Field Compaction to Improve Asphalt Mixture Durability*. Joint Transportation Research Program. Indiana Department of Transportation and Purdue University, West Lafayette, IN.

Hoegh, K., and Dai, S. 2017. *Asphalt Pavement Compaction Assessment using Ground Penetrating Radar-Arrays.* Paper presented at the Congress on Technical Advancement 2017, Duluth, MN.

Hoegh, K., Dai, S., Steiner, T., and Khazanovich, L. 2018. Enhanced Model for Continuous Dielectric-Based Asphalt Compaction Evaluation. *Transportation Research Record: Journal of the Transportation Research Board,* Vol. 2672, No. 26, pp. 144–154.

Hoegh, K., Khazanovich, L., Dai, S., and Yu, T. 2015. Evaluating Asphalt Concrete Air Void Variation via GPR Antenna Array Data. *Case Studies in Nondestructive Testing and Evaluation,* Vol. 3, pp. 27–33.

Hoegh, K., Roberts, R., Dai, S., and Zegeye Teshale, E. 2019. Toward Core-Free Pavement Compaction Evaluation: An Innovative Method Relating Asphalt Permittivity to Density. *Geosciences,* Vol. 9, No. 7, article 280.

Hoegh, K., Steiner, T., Zegeye Teshale, E., and Dai, S. 2020. Minnesota Department of Transportation Case Studies for Coreless Asphalt Pavement Compaction Assessment. *Transportation Research Record: Journal of the Transportation Research Board,* Vol. 2674, No. 2, pp. 291–301.

Horan, R., Chang, G., Xu, Q., and Gallivan, V. 2012. Improving Quality Control of Hot-Mix Asphalt Paving with Intelligent Compaction Technology. *Transportation Research Record: Journal of the Transportation Research Board,* No. 2268, pp. 82–91.

Huang, B., Shu, X., Chen, J., and Woods, M. 2010. Evaluation of Longitudinal Joint Construction Techniques for Asphalt Pavements in Tennessee. *Journal of Materials in Civil Engineering,* Vol. 22, No. 11, pp. 1112–1121.

Hughes, T., Davidson, J. K., and Cormier, A. 2009. *Performance of Warm Mix Technology in the Province of New Brunswick.* Paper presented at the Fifty-Fourth Annual Conference of the Canadian Technical Asphalt Association (CTAA), Moncton, New Brunswick.

Iowa DOT. 2015. *Developmental Specification 15036*: *Evaluation of Longitudinal Joint Quality for Flexible Paving Mixtures with Incentive/Disincentive*. Iowa Department of Transportation, Ames, IA. https://iowadot.gov/specifications/dev_specs/2015/DS-15036.pdf.

Kandhal, P., Ramirez, T., and Ingram, P. 2002. Evaluation of Eight Longitudinal Joint Construction Techniques for Asphalt Pavements in Pennsylvania. *Transportation Research Record: Journal of the Transportation Research Board,* No. 1813*,* pp. 87–94.

Kassem, E., Chowdhury, A., Scullion, T., and Masad, E. 2016. Application of Ground-Penetrating Radar in Measuring the Density of Asphalt Pavements and Its Relationship to Mechanical Properties. *International Journal of Pavement Engineering,* Vol. 17, No. 6, pp. 503–516.

Kassem, E., Masad, E., Chowdhury, A., and Claros, G. 2008. Influence of Field Compaction Pattern on Asphalt Pavement Uniformity (with discussion). *Journal of the Association of Asphalt Paving Technologists,* Vol. 77, pp. 257–298.

Khazanovich, L., Hoegh, K., Conway, R., and Dai, S. 2017. *Non-Destructive Evaluation of Bituminous Compaction Uniformity Using Rolling Density*. Second Strategic Highway Research Program, Washington, DC. http://shrp2.transportation.org/documents/R06C_NonDestructiveEval.pdf.

Kim, E. M.-Y. 2017. Evaluation of Asphalt Longitudinal Joint Construction and Practices in South Carolina. MS thesis. Clemson University, Clemson, SC. https://tigerprints.clemson.edu/all_theses/2735.

Kou, C., Xiao, P., Kang, A., Mikhailenko, P., Baaj, H., and Wu, Z. 2017. Protocol for the Morphology Analysis of SBS Polymer Modified Bitumen Images Obtained by Using Fluorescent Microscopy. *International Journal of Pavement Engineering*, Vol. 20, No. 5, pp. 585–591.

Les Davis, J., Rossiter, J. R., Darel, E., and Dawley, C. B. 1994. *Quantitative Measurement of Pavement Structures Using Radar.* Paper presented at the Fifth International Conferention on Ground Penetrating Radar, Kitchener, ON, Canada.

Lu, X., Isacsson, U., and Ekblad, J. 1999. Phase Separation of SBS Polymer Modified Bitumens. *Journal of Materials in Civil Engineering,* Vol. 11, No. 1, pp. 51–57.

Lu, X., Soenen, H., Heyrman, S., and Redelius, P. 2013. Durability of Polymer Modified Binders in Asphalt Pavements*. Proceedings of the XXVIII International Baltic Road Conference*, Vilnius, Lithuania.

Lu, X., Soenen, H., and Redelius, P. 2010. SBS Modified Bitumens: Does Their Morphology and Storage Stability Influence Asphalt Mix Performance. *Proceedings of the 11th International Society Asphalt Pavement (ISAP) International Conference on Asphalt Pavements*, Nagoya, Aichi, Japan, pp. 1604–1613.

Mallick, R. B., and Daniel, J. S. 2006. Development and Evaluation of a Field Permeameter as a Longitudinal Joint Quality Indicator. *International Journal of Pavement Engineering,* Vol. 7, No. 1, pp. 11–21.

Masad, E., Scarpas, A., Alipour, A., Rajagopal, K. R., and Kasbergen, C. 2016. Finite Element Modelling of Field Compaction of Hot-Mix Asphalt. Part I: Theory. *International Journal of Pavement Engineering,* Vol. 17, No. 1, pp. 13–23.

McDaniel, R. S., Shah, A., and Olek, J. 2012. *Longitudinal Joint Specifications and Performance*. Joint Transportation Research Program, Indiana Department of Transportation and Purdue University, West Lafayette, IN.

Minnesota Asphalt Pavement Association. 2014. Longitudinal Joint Construction. *October 2014 Paving Progress*. Minnesota Asphalt Pavement Association, St. Paul, MN.

MnDOT. 2016. *2360.Minnesota 2016 Standard Specifications: 3 D Compaction D.1 Maximum Density*. Minnesota Department of Transportation, St. Paul, MN.

Morey, R. M. 1998. *NCHRP Synthesis 255: Ground Penetrating Radar for Evaluating Subsurface Conditions for Transportation Facilities*. National Cooperative Highway Research Program, Washington, DC.

Mouillet, V., Lamontagne, J., Durrieu, F., Planche, J.-P., and Lapalu, L. 2008. Infrared Microscopy Investigation of Oxidation and Phase Evolution in Bitumen Modified with Polymers. *Fuel,* Vol. 87, No. 7, pp. 1270–1280.

Pavement Interactive. 2010. Longitudinal Joints – Part 2: Avoid Joint Failure. *RoadReady newsletter*. https://pavementinteractive.org/longitudinal-joints-part-2-avoid-joint-failure/.

Plati, C., and Loizos, A. 2013. Estimation of In Situ Density and Moisture Content in HMA Pavements Based on GPR Trace Reflection Amplitude Using Different Frequencies. *Journal of Applied Geophysics,* Vol. 97, pp. 3–10.

Polacco, G., Filippi, S., Merusi, F., and Stastna, G. 2015. A Review of the Fundamentals of Polymer-Modified Asphalts: Asphalt/Polymer Interactions and Principles of Compatibility. *Advances in Colloid and Interface Science,* Vol. 224, pp. 72–112.

Popik, M., Maser, K., and Holzschuher, C. 2010. Using high-speed ground penetrating radar for evaluation of asphalt density measurements. Paper presented at the Annual Conference and Exhibition of the Transportation Association of Canada, Halifax, NS, Canada.

Scullion, T., Lau, C., and Chen, Y. 1992. *Implementation of the Texas Ground Penetrating Radar System.* Texas Department of Transportation, Austin, TX.

Sebaaly, P., and Barrantes, J. 2004. *Development of a Joint Density Specification, Phase I: Literature Review and Test Plan*. Research Report #13L-1. Nevada Department of Transportation, Carson City, NV.

Sebaaly, P. E., Fernandez, G., and Hoffman, B. 2008. Evaluation of Construction Techniques for Longitudinal Joints in HMA Pavements (with discussion). *Journal of the Association of Asphalt Paving Technologists,* Vol. 77, pp. 143–182.

Shangguan, P., Al-Qadi, I., Coenen, A., and Zhao, S. 2016. Algorithm Development for the Application of Ground-Penetrating Radar on Asphalt Pavement Compaction Monitoring. *International Journal of Pavement Engineering,* Vol. 17, No. 3, pp. 189–200.

Soenen, H., Lu, X., and Redelius, P. 2008. The Morphology of Bitumen-SBS Blends by UV Microscopy. *Road Materials and Pavement Design,* Vol. 9, No. 1, pp. 97–110.

Soenen, H., Lu, X., and Redelius, P. 2009. The Morphology of SBS Modified Bitumen in Binders and in Asphalt Mix. In *Advanced Testing and Characterization of Bituminous Materials, Two Volume Set,* pp. 151–160. CRC Press, London, England.

Tran, N., Turner, P., and Shambley, J. 2016. *Enhanced Compaction to Improve Durability and Extend Pavement Service Life: A Literature Review*. National Center for Asphalt Technology, Auburn, AL.

Wagoner, M., Buttlar, W., and Paulino, G. 2005. Development of a Single-Edge Notched Beam Test for Asphalt Concrete Mixtures. *Journal of Testing and Evaluation,* Vol. 33, No. 6, pp. 452–460.

Wang, H., Wang, Z., Bennert, T., and Weed, R. 2016. Specification Limits and Pay Adjustment for Longitudinal Joint Density of Asphalt Pavements: Case Study in New Jersey. *Transportation Research Record: Journal of the Transportation Research Board,* No. 2573, pp. 98–106.

Wegan, V., and Brule, B. 1999. The Structure of Polymer Modified Binders and Corresponding Asphalt Mixtures. *Journal of the Association of Asphalt Paving Technologists,* Vol. 68, pp. 64–88.

Williams, S., Pervis, A., Bhupathiraju, L., and Porter, A. 2009. Methods for Evaluating Longitudinal Joint Quality in Asphalt Pavements. *Transportation Research Record: Journal of the Transportation Research Board,* No. 2098, pp. 113–123.

Williams, S. G. 2011. HMA Longitudinal Joint Evaluation and Construction. *TRC-0801 Final Report, AR.* University of Arkansas, Dept. of Civil Engineering, Fayetteville, AR.

Zhu, J., Lu, X., Balieu, R., and Kringos, N. 2016. Modelling and Numerical Simulation of Phase Separation in Polymer Modified Bitumen by Phase-Field Method. *Materials and Design,* Vol. 107, pp. 322–332.

Zhu, J., Balieu, R., Lu, X., and Kringos, N. 2017. Numerical Investigation on Phase Separation in Polymer-Modified Bitumen: Effect of Thermal Condition. *Journal of Materials Science,* Vol. 52, No. 11, pp. 6525–6541.

Zinke, S., and Mahoney, J. 2015. *Evaluation of Longitudinal Joint Density Specification on 2012 Polymer Modified Warm-Mix Asphalt Projects in Connecticut*. No. CT-2280-F-14-6. Connecticut. Dept. of Transportation. https://rosap.ntl.bts.gov/view/dot/30905.

APPENDIX A:
BITUMINOUS PLANT MIX DESIGN REPORTS

DEPARTMENT OF TRANSPORTATION

BITUMINOUS PLANT MIX DESIGN REPORT

District 7 Materials Lab
2151 Bassett Drive
Mankato, MN 56001
Phone: 507-304-6186
Fax: 507-304-6191

 # 07-2018-116

Date: 8/31/2018

THIS MIX DESIGN REPORT IS NOT VALID UNTIL PLANT NO. INDICATED BELOW IS CERTIFIED.

ENGINEER DAN FRANTA	**FOR** MNDOT D-7 MANKATO
PROJECT NUMBER SP 2208-113 TH 169	
CONTRACTOR SIGN.	

SPEC	2360 AFT
SPEC YEAR	2018
MIX TYPE	SPWEA430
AC GRADE	PG 58H-28

THIS MIXTURE HAS BEEN REVIEWED FOR VOLUMETRIC PROPERTIES ONLY, IT DOES NOT ASSURE THAT FIELD PLACEMENT AND COMPACTION REQUIREMENTS HAVE BEEN MET.

PLANT NO. **6-5002** - **2018A** JOB MIX FORMULA

Begin With Test Number		
SP	WE	501
SP		- - -

AFT Properties

Pbe	4.8
SA	26.7
Adj. AFT	9.2

Sieve Size (mm)	(in.)	Composite Formula	Broad Band			For Information Only Virgin Formula
25.0	(1)			–		
19.0	(3/4)	100		–		
12.5	(1/2)	100	100	–	100	
9.5	(3/8)	91	85	–	100	
4.75	(#4)	69	60	–	90	
2.36	(#8)	52	45	–	70	
1.18	(#16)	34		–		
0.600	(#30)	23		–		
0.300	(#50)	13		–		
0.150	(#100)	7		–		
0.075	(#200)	4.5	2.0	–	7.0	
Spec. Voids		3.0	2.0	–	4.0	
	% AC	5.5	5.1			%AC (NEW) 4.2
		(TOTAL)				

PERCENT PASSING

TM # 07-TM17-003 Indicates a Gyratory Density of 149.6 (lbs/ft3) at 90 Design Gyrations
Use of anti-strip required: No

	Pit	Source of Material	Total Sp. G	Minus #4 % Passing	Minus #4 Sp. G
9 %	24041	GLENVILLE 1/2" ADD ROCK	2.588	12 %	2.588
9 %	24041	GLENVILLE 1/2" NATURAL SAND	2.572	89 %	2.572
22 %	93018	Northwood 1/2" Add Rock	2.710	19 %	2.692
20 %	93041	FALKSTONE MANSAND	2.725	100 %	2.725
10 %	93018	NORTHWOOD MANSAND	2.727	100 %	2.727
%				%	
15 %		GLENVILLE RAP	2.620	73 %	2.620
15 %		GLENVILLE MILLINGS	2.608	76 %	2.608
		Mix Aggregate Specific Gravity at the Listed Percentages =	**2.661**		**2.663**

FOR LAB INFORMATION ONLY: LAB COMPACTION TEMP. RANGE = 247-255 °F

Remarks: REISSUE OF 06-2018-035 TO A SPWEA430 MIX WITH SLIGHT AGGREGATE CHANGES TO MEET 3.0 VOIDS. AC SPG = 1.035 SET CORRECTION FACTOR WITH FIRST VERIFICATION SAMPLE.

Mix Design Reviewed by:

Mark D. Schoeb

Mix Design Specialist

cc: **Dist Mat'ls Eng.** - CHARLES KREMER
Contractor - Ulland Bros.
DAN FRANTA BOLTON & MENK
Dist Lab File-2

07-2018-116 Ver. 1

DEPARTMENT OF TRANSPORTATION

BITUMINOUS PLANT MIX DESIGN REPORT

District 7 Materials Lab
2151 Bassett Drive
Mankato, MN 56001
Phone: 507-304-6186
Fax: 507-304-6191

 # 07-2018-040

Date: 5/31/2018

THIS MIX DESIGN REPORT IS NOT VALID UNTIL PLANT NO. INDICATED BELOW IS CERTIFIED.

ENGINEER DAN FRANTA B & M	**FOR** MNDOT D-7 MANKATO
PROJECT NUMBER SP 0704-100 TH 22	
CONTRACTOR SIGN.	

SPEC	2360 AFT
SPEC YEAR	2016
MIX TYPE	SPWEB440
AC GRADE	58H-34

THIS MIXTURE HAS BEEN REVIEWED FOR VOLUMETRIC PROPERTIES ONLY, IT DOES NOT ASSURE THAT FIELD PLACEMENT AND COMPACTION REQUIREMENTS HAVE BEEN MET.

PLANT NO. **974101** - **2018A** JOB MIX FORMULA

Begin With Test Number

SP	WE	001
- -	- -	- - -

AFT Properties

Pbe	4.8
SA	21.2
Adj. AFT	11.2

Sieve Size (mm) (in.)	Composite Formula	Broad Band		For Information Only Virgin Formula
25.0 (1)				
19.0 (3/4)	100	100	100	
12.5 (1/2)	91	85	100	
9.5 (3/8)	82	35	90	
4.75 (#4)	55	30	80	
2.36 (#8)	41	25	65	
1.18 (#16)	36			
0.600 (#30)	24			
0.300 (#50)	11			
0.150 (#100)	4			
0.075 (#200)	2.8	2.0	7.0	
Spec. Voids	4.0	3.0	5.0	
% AC	5.4	5.0		%AC (NEW) 4.4
	(TOTAL)			PERCENT PASSING

TM # 07-TM15-0019 Indicates a Gyratory Density of 146.2 (lbs/ft3) at 90 Design Gyrations
Use of anti-strip required: No

	Pit	Source of Material	Total Sp. G	Minus #4 % Passing	Minus #4 Sp. G
24 %	52003	NEW ULM QUARTZITE QUARRY 3/4 ROCK	2.630	4 %	2.630
0 %	40037	Davis 3/8" WASH ROCK	2.584	31 %	2.550
10 %	40037	Davis Wash Sand	2.582	100 %	2.582
35 %	52003	NEW ULM QUARTZITE WASHED MANSAND (NEW)	2.631	87 %	2.631
0 %	52003	NEW ULM QUARTZITE 3/8" W/ FINES	2.617	98 %	2.617
10 %	52003	NEW ULM QUARTZITE FA 2 1/2	2.634	23 %	2.639
0 %	RAS	MANUFACTURE WASTE SHINGLES	2.650	100 %	2.650
21 %	RAP	SMC-RBA PLANT RAP	2.624	81 %	2.624
		Mix Aggregate Specific Gravity at the Listed Percentages =	**2.625**		**2.621**

FOR LAB INFORMATION ONLY: LAB COMPACTION TEMP. RANGE = 260-275 °F

Remarks: ROLLOVER OF 07-2018-030 FOR DIFFERENT MNDOT PROJECT. AC SPG = 1.032 EVOTHERM ADDED FOR COMPACTION AID.

Mix Design Reviewed by:

Mark D. Schoeb

Mix Design Specialist

07-2018-040 Ver. 2

cc: **Dist Mat'ls Eng. -** CHARLES KREMER
Contractor - SMC/RBA
DAN FRANTA BOLTON & MENK
Dist Lab File-2

APPENDIX B:
FIELD SURVEY REPORT

DEPARTMENT OF TRANSPORTATION

MnDOT Office of Materials and Road Research
Mailstop 645
1400 Gervais Avenue
Maplewood, MN 55109

Internal Memo

Date: 3/29/19

To: **File**

From: **Ed Johnson**

Phone: **651-366-5465**

RE: Field review of J-Band installations – D7, T9PR8999

J-Band longitudinal joint treatment was installed on two MnDOT District 7 paving projects during 2018. The two projects are subjects of a Minnesota LRRB study (Dr. Chris Williams – Iowa State University). On 3/25/19 the two projects were visited by Ed Johnson - MnDOT Office of Materials and Road Research.

If was found that both installations suffered little damage during the first winter of service.

Observations:

US TH 169 North of Blue Earth, MN – RP 12.678 to 13.605

- Centerline rumbles on much of J-Band.
- Generally did not notice anything out of ordinary. several segments with longitudinal joint showing lost material. Material loss limited to top layer of rock: 1 in. wide and 0.5 in. deep. Otherwise in good condition. Good condition at south end of application (FIGURE 1)
- Some locations showed slight material loss in the longitudinal joint near middle of application (FIGURE 2)
- Longitudinal Joint Adhesive was clearly visible in those areas (FIGURE 3)

Figure 1 J-Band US169, Good condition.

Figure 2 J-Band US 169. Some material loss along joint.

Figure 3 Longitudinal Joint Adhesive US 169. Good condition.

MN TH 22 North of Beauford, MN – RP 43.618 to 44.614

- Centerline rumbles on much of J-Band.
- Generally did not notice anything out of ordinary
    - Good condition at south end of application (FIGURE 4)
    - Good condition at north end of application (FIGURE 5)
    - Control north of applicaton was in good condition.

Figure 4 TH 22 J-Band. Good condition.

Figure 5 TH 22 J-Band. Good condition.

APPENDIX C:
IMAGES


09/17/2018 11:42


09/17/2018 11:44


09/17/2018 11:46

APPENDIX D:
LABORATORY RESULTS

Joint Bond Energy at -24°C, DCT Test Results

Samples, control section	Fracture energy, control section (j/m^2)	Samples, VRAM section	Fracture energy, VRAM section (j/m^2)
1	883.0	A	1195.0
2	760.0	B	737.5
3	938.8	C	775.0
Average	860.6		902.5

Cracking Resistance, SCB Test Results

Samples, control section	Fracture energy, control section (j/m^2)	Samples, VRAM section	Fracture energy, VRAM section (j/m^2)
1	590.1	A	886.9
2	638.1	B	759.8
3	508.8	C	700.3
Average	579.0		782.3